KfK 5235
Oktober 1993

State-of-the-Art of High Power Gyro-Devices and Free Electron Masers

M. Thumm
Institut für Technische Physik
Projekt Kernfusion

Kernforschungszentrum Karlsruhe

KERNFORSCHUNGSZENTRUM KARLSRUHE

Institut für Technische Physik

Projekt Kernfusion

KfK 5235

STATE-OF-THE-ART OF HIGH POWER GYRO-DEVICES AND FREE ELECTRON MASERS

M. Thumm

Kernforschungszentrum Karlsruhe GmbH, Karlsruhe

Kernforschungszentrum Karlsruhe GmbH
Postfach 3640, 76021 Karlsruhe

ISSN 0303-4003

STATE-OF-THE-ART OF HIGH POWER GYRO-DEVICES AND FREE ELECTRON MASERS

Abstract

At present, gyrotron oscillators are mainly used as high power millimeter wave sources for electron cyclotron resonance heating (ECRH) and diagnostics of magnetically confined plasmas for generation of energy by controlled thermonuclear fusion. 140 GHz gyrotrons with output power P_{out} = 0.58 MW, pulse length τ = 2.0 s and efficiency η = 34 % are commercially available. Diagnostic gyrotrons deliver P_{out} = 40 kW with τ = 40 μs at frequencies up to 650 GHz ($\eta \geq$ 4 %). Recently, gyrotron oscillators have also been successfully used in material processing and plasma chemistry. Such technological applications require gyrotrons with the following parameters: f $\geq$ 28 GHz , P_{out} = 10-30 kW, CW, $\eta \geq$ 30 %. This paper reports on achievements and problems related to the development of very high power mm-wave gyrotrons for long pulse or CW operation and describes the microwave technological pecularities of the different development steps. In addition, this work gives a short overview of the present development of gyrotrons for technological applications, quasi-optical gyrotrons, cyclotron autoresonance masers (CARMs), gyro-klystrons, gyro-TWT amplifiers, gyro-BWO's and free electron masers (FEMs). The most impressive FEM output parameters are: P_{out} = 2GW, τ = 20 ns, η = 13 % at 140 GHz (LLNL) and P_{out} = 15 kW, τ = 20 μs, η = 5 % in the range from 120 to 900 GHz (UCSB).

ENTWICKLUNGSSTAND VON HOCHLEISTUNGS-GYRO-RÖHREN UND FREI-ELEKTRONEN-MASERN

Übersicht

Gyrotronoszillatoren werden derzeit vorwiegend als Hochleistungsmillimeterwellenquellen für die Elektron-Zyklotron-Resonanzheizung (ECRH) und Diagnostik von magnetisch eingeschlossenen Plasmen zur Erforschung der Energiegewinnung durch kontrollierte Kernfusion eingesetzt. 140 GHz Gyrotrons mit einer Ausgangsleistung von P_{out} = 0.58 MW bei Pulslängen von τ = 2.0 s und Wirkungsgraden von η = 34% sind kommerziell erhältlich. Gyrotrons zur Plasmadiagnostik erreichen Frequenzen bis zu 650 GHz bei P_{out} = 40 kW und τ = 40 μs ($\eta \geq$ 4 %). In jüngster Zeit jedoch finden Gyrotronoszillatoren auch für technologische Prozesse und in der Plasmachemie erfolgreich Verwendung. Dabei werden Röhren mit folgenden Parametern eingesetzt: f $\geq$ 28 GHz, P_{out} = 10-30 kW, CW, $\eta \geq$ 30 %. In diesem Beitrag wird auf den aktuellen Stand und die Probleme bei der Entwicklung von Hochleistungs-mm-Wellen-Gyrotrons für Langpuls- und Dauerstrichbetrieb sowie auf die mikrowellentechnischen Besonderheiten der einzelnen Entwicklungsphasen eingegangen. Außerdem wird auch kurz über den neuesten Stand der Entwicklung von Gyrotrons für technologische Anwendungen, quasi-optischen Gyrotrons, Zyklotron-Autoresonanz-Masern (CARMs), Gyroklystrons, Gyro-TWT-Verstärkern, Gyro-Rückwärtswellenoszillatoren (BWOs) und Frei-Elektronen-Maser (FEM) berichtet. FEM-Rekordausgangsparameter sind hier: P_{out} = 2 GW, τ = 20 ns, η = 13 % bei 140 GHz (LLNL) und P_{out} = 15 kW, τ = 20 μs, η = 5 % im Bereich von 120 bis 900 GHz (UCSB).

Contents

1	**Introduction**		**1**
2	**Classification of Fast-Wave Microwave Sources**		**2**
3	**Dispersion Diagrams of Fast Cyclotron Mode Interaction**		**3**
	3.1	Gyrotron oscillator and gyroklystron amplifier	4
	3.2	Cyclotron autoresonance maser (CARM)	6
	3.3	Gyro-TWT (travelling wave tube) amplifier	8
	3.4	Gyro-BWO (backward wave oscillator)	8
4	**Gyrotron Oscillators for Plasma Heating**		**9**
5	**Very High Frequency Gyrotron Oscillators**		**18**
6	**Gyrotrons for Technological Applications**		**20**
7	**Quasi-Optical Gyrotrons**		**21**
8	**Cyclotron Autoresonance Masers (CARMs)**		**22**
9	**Gyroklystrons, Gyro-TWTs, Gyro-BWOs and other Gyro-Devices**		**23**
10	**Free Electron Masers (FEMs)**		**25**
	10.1	Potentialities	25
	10.2	Accelerator options and key issues	25
	10.3	The FOM-Fusion-FEM	27
11	**Comparison of Gyrotron and FEM for Nuclear Fusion**		**30**
	Acknowledgments		**31**
	References		**32**

1 Introduction

The possible applications of gyrotron oscillators and other cyclotron-resonance maser (CRM) fast wave devices span a wide range of technologies. The plasma physics community has already taken advantage of recent advances in producing high power micro- and millimeter waves in the areas of RF plasma heating, for magnetic confinement fusion studies, as lower hybrid heating (1-8 GHz) and electron cyclotron resonance heating (28-140 GHz), plasma production for numerous different processes and plasma diagnostic measurements as collective Thomson scattering or heat pulse propagation experiments. Other applications which await the development of novel high power sources include deep space and specialized satellite communication, high resolution Doppler radar, radar ranging and imaging in atmospheric and planetary science, drivers for next-generation high-gradient linear accelerators, nonlinear spectroscopy and technological applications.

Most work on CRM devices has investigated the conventional gyrotron oscillator (gyromonotron) [1-3] in which the wave vector of the radiation in an open-ended, irregular cylindrical waveguide cavity is transverse to the direction of the applied magnetic field, resulting in radiation near the electron cyclotron frequency or on one of its harmonics. Long pulse and CW gyrotron oscillators delivering output powers of 100-400 kW at frequencies between 28 and 84 GHz have been used very successfully in thermonuclear fusion research for plasma ionization and start-up, electron cyclotron resonance heating (ECRH) and local current density profile control by noninductive electron cyclotron current drive (ECCD) at power levels up to 4 MW.

ECRH has become a well-established heating method for both tokamaks [4] and stellarators [5]. The confining magnetic fields in present day fusion devices are in the range of B_o=1-3.5 Tesla. As fusion machines become larger and operate at higher magnetic fields ($B \geqq 5T$) and higher plasma densities in steady state, it is necessary to develop CW gyrotrons that operate at both higher frequencies and higher mm-wave output powers. The requirements of the projected tokamak experiment ITER (International Thermonuclear Experimental Reactor) and of the planned new stellarator (W7-X) at the Max-Planck-Institut für Plasmaphysik in Garching are between 10 and 30 MW at frequencies around 140 GHz [6]. This suggests that mm-wave gyrotrons that generate output power of at least 1 MW, CW, per unit are required. Since efficient ECRH needs axisymmetric, narrow, pencil-like mm-wave beams with well defined polarization (linear or elliptical), single mode gyrotron emission is necessary in order to generate a TEM_{00} Gaussian beam mode. Single mode 110-140 GHz gyromonotrons capable of high average power 0.5 - 1 MW per tube, CW, are currently under development. There has been continuous progress towards higher frequency and power but the main issues are still the long pulse or CW operation and the appropriate mm-wave vacuum window. The availability of sources with fast frequency tunability would permit the use of a simple, non-steerable mirror antenna at the plasma torus for local current drive experiments [6]. Slow frequency tuning has been shown to be possible on quasi-optical Fabry-Perot cavity gyrotrons [7] as well as on cylindrical cavity gyrotrons with step tuning (different working modes) [8, 9].

This work reports on the status and future prospects of the development of gyrotron oscillators for ECRH but also refers to the development of pulsed very high frequency gyromonotrons for active plasma diagnostics [10].

Recently, gyrotron oscillators also are successfully utilized in material processing (e.g. advanced ceramic sintering, surface hardening or dielectric coating of metals and alloys) as well as in plasma chemistry [11]. The use of gyrotrons for such technological applications appears to be of interest if one can realize a relatively simple, low cost device which is easy in service (such as a magnetron). Gyrotrons with low magnetic field (operated at the 2nd harmonic of the electron cyclotron frequency), low anode voltage, high efficiency and long lifetime are under development. The state of the art in this area is also briefly reviewed here.

The next generation of high-energy physics accelerators and the next frontier in understanding of elementary particles is based on the super collider. For linear electron-positron colliders that will reach center-of-mass energies of about 1 TeV it is thought that sources at 17 to 35 GHz with P_{out} = 300 MW, τ = 0.2 µs and characteristics that will allow approximately 1000 pulses per second will be necessary as drivers [12]. These must be phase-coherent devices, which can be either amplifiers or phase locked oscillators. Therefore this contribution gives a short overview of the present development status of free electron masers (FEM), cyclotron autoresonance masers (CARM), gyrotron travelling wave tube amplifiers (Gyro-TWT) and gyroklystrons for such purposes as well as of broadband gyrotron backward wave oscillators (Gyro-BWO) for use as drivers for FEM amplifiers.

2 Classification of fast-wave microwave sources

Fast-wave devices in which the phase velocity v_{ph} of the electromagnetic wave is greater than the speed of light c, generate or amplify coherent electromagnetic radiation by stimulated emission of bremsstrahlung from a beam of relativistic electrons. The electrons radiate because they undergo oscillations transverse to the direction of beam motion by the action of an external force (field). For such waves the electric field is mainly transverse to the propagation direction.

The condition for coherent radiation is that the contribution from the electrons reinforces the original emitted radiation in the oscillator or the incident electromagnetic wave in the amplifier. This condition is satisfied if a bunching mechanism exists to create electron density variations of a size comparable to the wavelength of the imposed electromagnetic wave. To achieve such a mechanism, a resonance condition must be satisfied between the periodic motion of the electrons and the electromagnetic wave in the interaction region [13]

$$\omega - k_z v_z \cong s\Omega \quad , \quad s = 1,2,\ldots \qquad (k_z v_z = \text{Doppler term}) \tag{1}$$

here ω and k_z are the electromagnetic wave frequency and characteristic axial wavenumber, respectively, v_z is the translational electron drift velocity, Ω is an effective frequency, which is associated with macroscopic oscillatory motion of the electrons, and s is the harmonic number.

In the electron cyclotron resonance maser (CRM), electromagnetic energy is radiated by relativistic electrons gyrating along an external longitudinal magnetic field. In this case, the effective frequency Ω corresponds to the relativistic electron cyclotron frequency:

$$\Omega_c = \Omega_{co}/\gamma \quad \text{with} \quad \Omega_{co} = eB_o/m_o \quad \text{and} \quad \gamma = [1-\ (v/c)^2]^{-1/2} \tag{2}$$

where e and m_o are the charge and rest mass of an electron, γ is the relativistic factor, and B_o is the magnitude of the guide magnetic field. A group of relativistic electrons gyrating in a strong magnetic field will radiate coherently due to bunching caused by the relativistic mass dependence of their gyration frequency. Bunching is achieved because, as an electron loses energy, its relativistic mass decreases and it thus gyrates faster. The consequence is that a small amplitude wave's electric field, while extracting energy from the particles, causes them to become bunched in gyration phase and reinforces the existing wave electric field. The strength of the magnetic field determines the value of the radiation frequency.

In the case of a spacially periodic magnetic or electric field (undulator/wiggler), the oscillation frequency Ω_b (bounce frequency) is proportional to the ratio of the electron beam velocity v_z to the field spatial period λ_w. Thus,

$$\Omega_b = k_w v_z \quad , \quad k_w = 2\pi/\lambda_w \tag{3}$$

The operating frequency of such devices, an example of which is the FEM [13-15], is determined by the condition that an electron in its rest frame "observes" both the radiation and the periodic external force at the same frequency. If the electron beam is highly relativistic, ($v_{ph} \cong v_z \cong c$) the radiation will have a much shorter wavelength than the external force in the laboratory frame ($\lambda \cong \lambda_w/2\gamma^2$ so that $\omega \cong 2\gamma^2\,\Omega_b$). Therefore, FEMs are capable of generating electromagnetic waves of very short wavelength determined by the relativistic Doppler effect. The bunching of the electrons in FEMs is due to the perturbation of the beam electrons by the ponderomotive wave, a wave caused by "beating" of the electromagnetic wave with the spatially periodic wiggler field.

In the case of the CRMs and FEMs, unlike most conventional microwave sources and lasers, the radiation wavelength is not determined by the characteristic size of the interaction region. Such fast wave devices require no periodically rippled walls or dielectric loading and can instead use a simple hollow-pipe, oversized waveguide as a circuit. These devices are capable of producing very high power radiation at cm-, mm-, and submillimeter wavelengths.

3 Dispersion diagrams of fast cyclotron mode interaction

Many configurations can be used to produce coherent radiation based on the electron cyclotron maser instability. The departure point for designs based on a particular concept is the wave-particle interaction. Dispersion diagrams, also called ω-k_z plots or Brillouin diagrams (e.g. Fig. 3) [16], show the region of cyclotron interaction (maximum gain of the instability) between an electromagnetic mode and a fast electron cyclotron mode (fundamental or harmonic) as an intersection of the waveguide mode dispersion curve (hyperbola):

$$\omega^2 = k_z^2 c^2 + k_\perp^2 c^2 \tag{4}$$

with the beam-wave resonance line (straight) given by eq. (1). In the case of a device with cylindrical resonator the perpendicular wavenumber is given by $k_\perp = X_{mn} / R_o$ where X_{mn} is the nth root of the corresponding Bessel function (TM_{mn} modes) or derivative (TE_{mn} modes) and R_o is the waveguide radius. Phase velocity synchronism of the two waves is given in the intersection region. The interaction can result in a device that is either an oscillator or an amplifier. In the following subsections, the different CRM devices are classified according to their dispersion diagrams.

3.1 Gyrotron oscillator and gyroklystron amplifier

Gyrotron oscillators and gyroklystrons are devices which usually utilize only weakly relativistic electron beams (<100 kV) with high transverse momentum (pitch angle $\alpha = v_\perp/v_z > 1$). The wavevector of the radiation in the cavity is transverse to the direction of the external magnetic field ($k_\perp >> k_z$, and the Doppler shift is small) resulting according to eqs. (1) and (2) in radiation near the electron cyclotron frequency or on one of its harmonics:

$$\omega \cong s\Omega_c \ , \qquad s = 1,2,... \qquad (5)$$

In the case of cylindrical cavity tubes (see Figs. 1 and 2) the operating mode is close to cutoff ($v_{ph} = \omega/k_z >> c$) and the frequency mismatch $\omega - s\Omega_c$ is small but positive in order to achieve correct phasing, i.e. keeping electron bunches in the retarding phase. The Doppler term $k_z v_z$ is of the order of the gain width and is small compared with the radiation frequency. The dispersion diagrams of fundamental and harmonic gyrotrons are illustrated in Figs. 3 and 4, respectively. The velocity of light line is determined by $\omega = ck_z$. For given values of γ and R_o, a mode represented by X_{mn} and oscillating at frequency ω is only excited over a narrow range of B_o. By variation of the magnetic field, a sequence of discrete modes can be excited. The frequency scaling is determined by the value of B_o/γ. Cyclotron harmonic operation reduces the required magnetic field for a given frequency by the factor s. The predicted efficiency for gyrotrons operating at higher harmonics (s = 2 and 3) are comparable with those operating at the fundamental frequency [16].

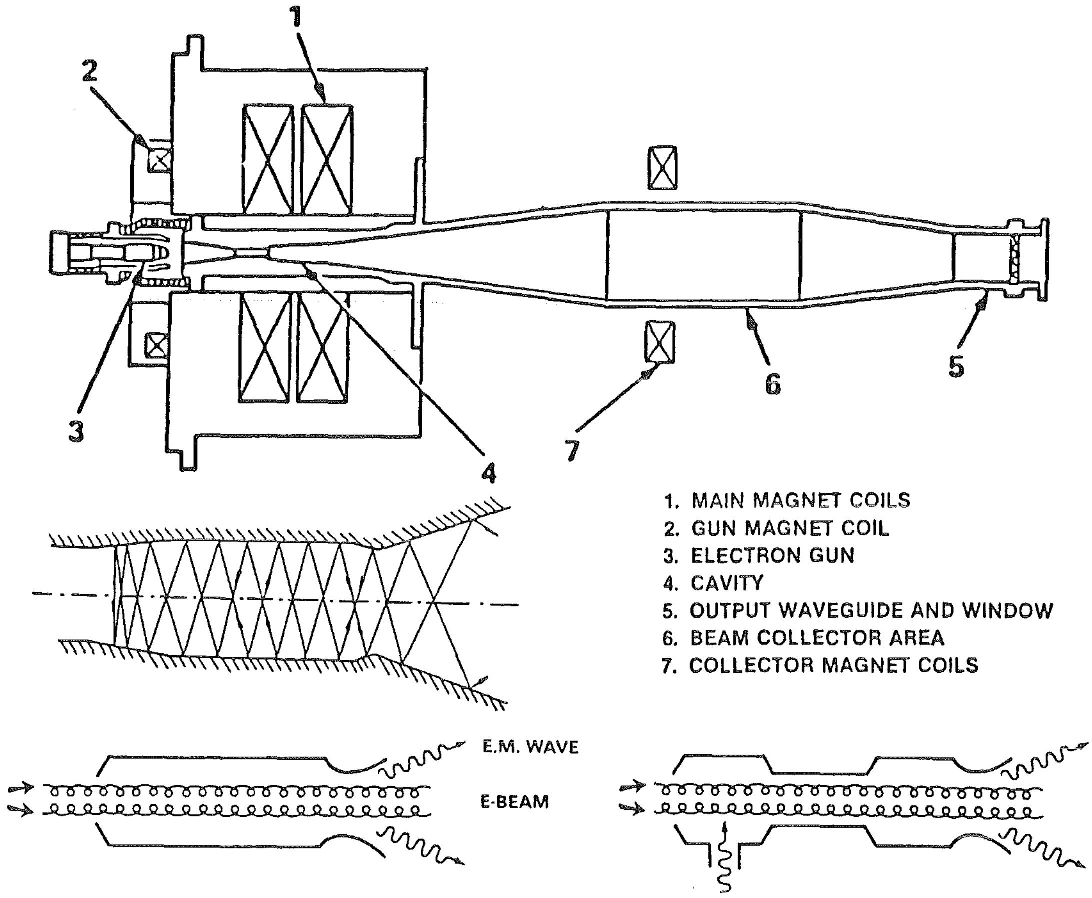

Fig. 1. Schematic of VARIAN CW gyrotron oscillator [2] and scheme of irregular waveguide cavities of gyromonotron oscillator (left) and gyroklystron amplifier [16].

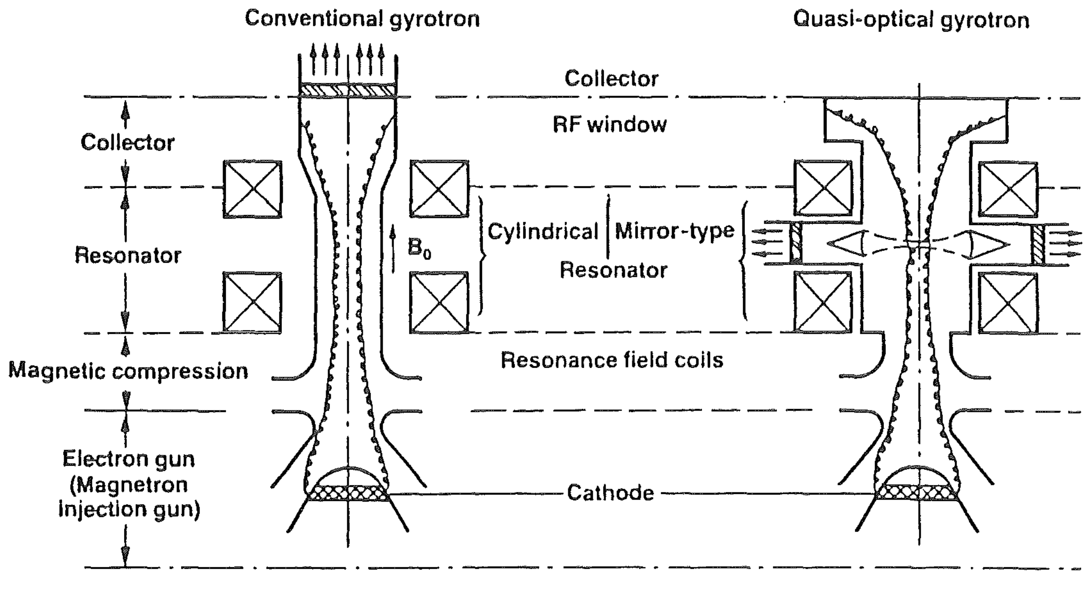

Fig. 2 Principle of a conventional gyrotron with cylindrical resonator and of a quasi-optical gyrotron with mirror resonator [7].

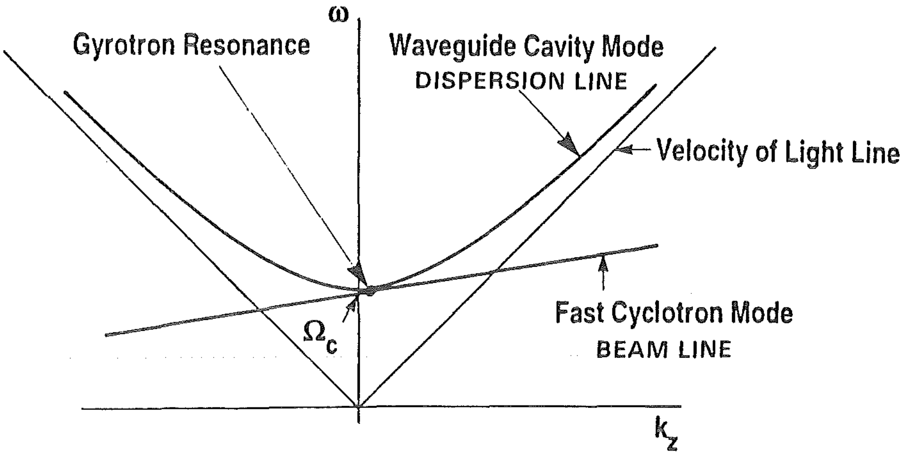

Fig. 3 Dispersion diagram of gyrotron oscillator (fundamental resonance)

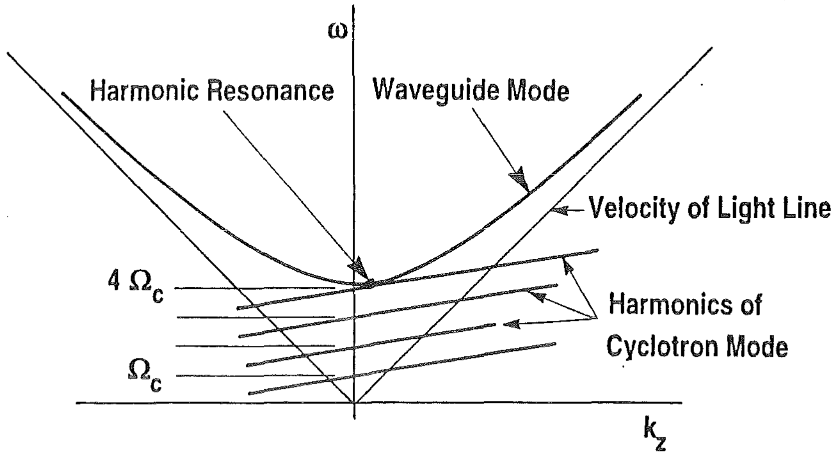

Fig. 4 Dispersion diagram of harmonic frequency gyrotron oscillator

3.2 Cyclotron autoresonance maser (CARM)

In a gyrotron with a highly relativistic beam, an efficient interaction will lead to an average energy loss in the order of the initial electron energy. As a result, the change in the gyrofrequency will be much greater than in the mildly relativistic case. It is therefore desirable to identify the condition under which an electron that loses energy remains in synchronism with the RF field. A possibility for achieving such synchronism is to utilize the interaction of electrons with electromagnetic waves propagating at a phase velocity close to the speed of light in the direction of the magnetic field. In this case, the Doppler shift term $k_z v_z$ is large, and the appropriate resonance condition is

$$\omega \cong k_z v_z + s\Omega_c \tag{6}$$

If $v_{ph} \cong c$, the increase in cyclotron frequency due to extraction of beam energy (decrease of γ) nearly compensates the decrease in the Doppler shifted term. Therefore, if the resonance condition is initially fulfilled, it will continue to be satisfied during the interaction. This phenomenon is called autoresonance, and the cyclotron maser devices operating in the relativistic Doppler-shifted regime are called cyclotron autoresonance masers [13]. Fig. 5

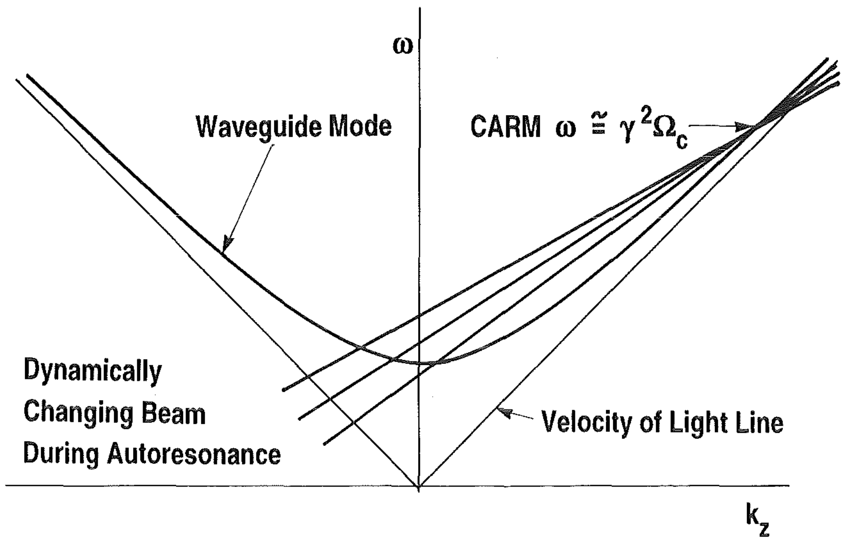

Fig. 5 Dispersion diagram of the cyclotron autoresonance maser (CARM).

shows how the Brillouin diagram of the fast cyclotron wave changes during the autoresonance interaction such that the working frequency ω remains constant even though both Ω_c and v_z are changing. The CARM interaction corresponds to the upper intersection and is based on the same instability mechanism as that of the gyrotron but operated far above cutoff. The instability is convective, so feedback, e.g. by a Bragg resonator (see Fig. 6) [13] is required for an oscillator and it is necessary to carefully discriminate against the other interactions corresponding to the lower frequency intersection in the dispersion diagram Fig. 5. The problem can be alleviated by employing the fundamental TE_{11} or (HE_{11} hybrid mode) and properly choosing system parameters to be within the stability limit. There is a large Doppler frequency upshift of the output over that of the gyrotron ($\omega \cong \gamma^2\Omega_c$) permitting a considerably reduced magnetic field B_0. Since the axial bunching mechanism can substantially offset the azimuthal bunching the total energy of the beam and not only the transverse component is vailable for RF conversion.

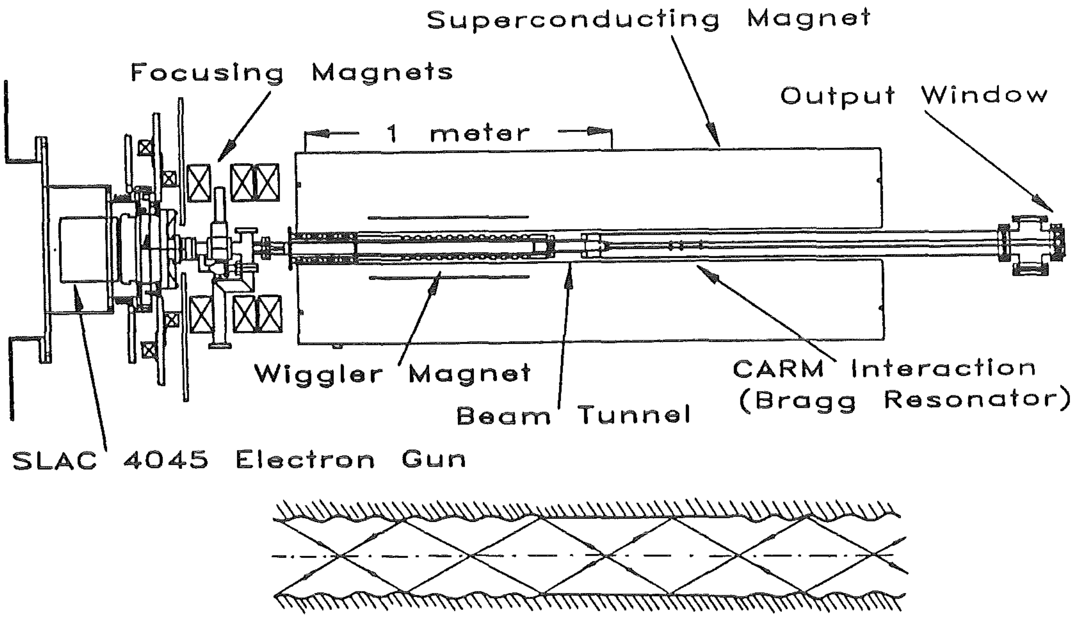

Fig. 6 Schematic of the long-pulse MIT CARM oscillator experiment [17] and scheme of a Bragg resonator [13].

In contrast to the gyrotron the CARM has an electron beam with low to moderate pitch angle ($\alpha < 0.7$). The efficiency of CARMs is extremely sensitive to spread in the parallel beam velocity. The velocity spread $\Delta v_z/v_z$ must be lower than 1% to achieve full theoretically expected efficiency of 40%. [13, 17].

3.3 Gyro-TWT (travelling wave tube) amplifier

From the theoretical point of view, the gyro-TWT differs from the CARM only in regimes of operation. The gyro-TWT utilizes a moderately relativistic electron beam to interact with a fast waveguide mode near the grazing intersection of the frequency versus wavenumber plot (see Fig. 7) where the resonance line is tangent to the electromagnetic mode. This produces high gain and efficiency because the phase velocities of the two modes are

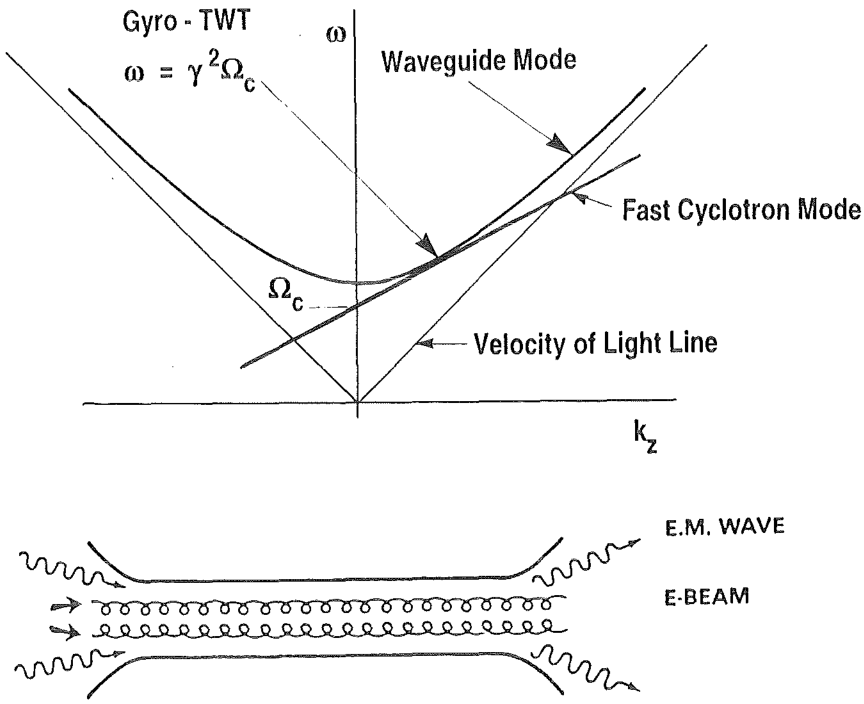

Fig. 7 Dispersion diagram and scheme of interaction circuit of Gyro-TWT amplifier.

nearly matched and the group velocity of the waveguide mode is nearly equal to v_z. In the gyro-TWT regime ($\omega/k_z >> c$), the axial bunching mechanism is too weak to be of any significance. To benefit from autoresonance, the cutoff frequency should be reduced relative to the cyclotron frequency. The circuit employed in a gyro-TWT consists simply of an unloaded waveguide. Since no resonant structures are present, the gyro-TWT is potentially capable of much larger bandwidth than a gyroklystron and thus can be used as output amplifier in mm-wave radar communication systems.

3.4 Gyro-BWO (backward wave oscillator)

If the electron beam and/or magnetic field is adjusted so that the straight fast-wave beam line crosses the negative k_z-branch of the waveguide mode hyperbola (see Fig. 8) then an absolute instability (internal feedback) with a "backward wave" occurs. In the gyro-BWO the

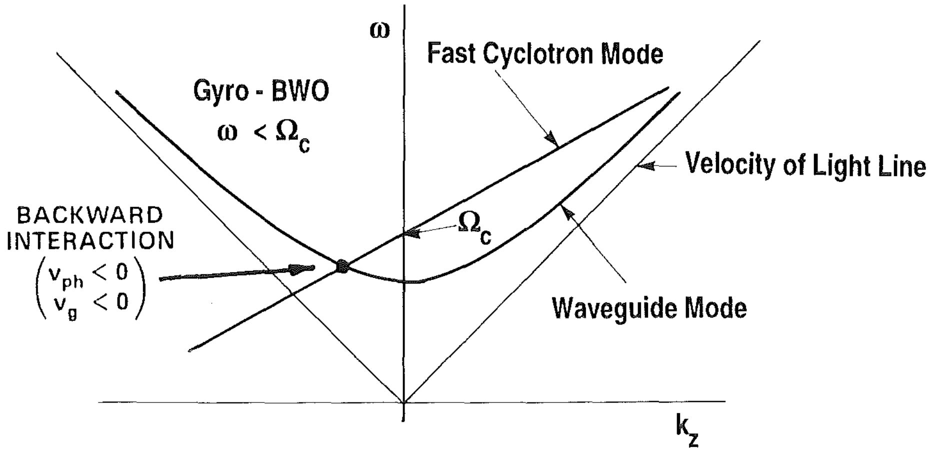

Fig. 8 Dispersion diagram of Gyro-BWO

frequency of operation is now governed by the slope of the line, which is a function of v_z, and thus of the beam acceleration voltage U_{beam}. Consequently, just as in the case of other BWOs (e.g. carcinotron), the frequency of oscillations can be continuously changed very fast over a broad range, using U_{beam} in place of B_0. However, there is a Doppler down shift in frequency ($\Omega_c/2 < \omega < \Omega_c$), so that very high magnetic fields are required for high frequency operation.

4 Gyrotron oscillators for plasma heating

Long-pulse and CW gyromonotrons utilizing open-ended cylindrical resonators which generate output powers of 100 - 400 kW per unit, at frequencies between 28 and 84 GHz, have been used very successfully for plasma formation, electron cyclotron resonance heating (ECRH) and local current density profile control by noninductive current drive (ECCD) in tokamaks [4] and stellarators [5]. Gyrotron complexes with total power of up to 4 MW are used [10]. Table I summarizes the capabilities and performance parameters of such gyrotrons together with the features of 8 GHz gyrotron oscillators for lower hybrid heating and current drive in tokamak plasmas. The confining toroidal magnetic fields in present day fusion machines are in the range of $B_0=1\text{-}3.5$ Tesla. As experimental devices become larger and operate at higher magnetic fields (B=5T) and higher plasma densities ($n_{e0}=1\text{-}2\cdot 10^{20}/m^3$) in steady state, present and forthcoming ECH requirements call for gyrotron output powers of at least 1 MW, CW at frequencies ranging from 100-180 GHz (the reference frequency is 140 GHz [6]). Since efficient ECRH and ECCD needs axisymmetric, narrow, pencil-like mm-wave beams with well defined polarization, single mode emission is necessary in order to generate a TEM_{00} Gaussian beam mode at the plasma torus launching antenna [6, 23].

Single mode mm-wave gyrotron oscillators capable of high average power, 0.5-1 MW per tube, in longpulse or CW operation, are currently under development in several scientific and industrial laboratories. The present state of the art is given in Table II. Some experimental results are shown in Figs. 9 and 10.

Institution		Frequency [GHz]	Mode cavity	Mode output	Power [MW]	Efficiency [%]	Pulse length [s]
ABB, Baden	[18]	8	TE_{01}	TE_{01}	0.35	35	0.5
		39	TE_{02}	TE_{02}	0.25	42	0.1
HUGHES, Torrance	[16]	60	TE_{02}	TE_{02}	0.2	35	0.1
NRL, Washington D.C	[16]	35	TE_{01}	TE_{01}	0.15	31	0.02
IEAS, Beijing	[19]	34.3 ($2\Omega_c$)	$TE_{02/03}$	TE_{03}	0.2	30	0.02
		36.5 ($2\Omega_c$)	TE_{02}	TE_{02}	0.1	25	0.02
PHILIPS, Hamburg	[3]	70	TE_{02}	TE_{02}	0.14	30	CW
SALUT, IAP,		28	TE_{42}	TEM_{00}	0.5	30	0.1
Nizhny Novgorod	[9,10]	37.5		TEM_{00}	0.5	35	0.1
		53.2	TE_{83}	TEM_{00}	0.5	41.7	0.1
		75 , 83	$TE_{11,3}$	TEM_{00}	0.5	37	1.5
THOMSON TE,		8	TE_{51}	TE_{51}	1.0	45	1.0
Velizy	[20]	35	TE_{02}	TE_{02}	0.2	43	0.15
TOSHIBA,		28	TE_{02}	TE_{02}	0.2	35	0.075
Shimoishigami	[21]	41 , 56	TE_{02}	TE_{02}	0.2	30	0.1
VARIAN,		8	TE_{21}	$TE_{10}^{\square}$	0.5	33	1.0
Palo Alto	[2,22]	28	TE_{02}	TE_{02}	0.34	37	CW
		35	TE_{02}	TE_{02}	0.2	35	CW
		53.2, 56, 60	$TE_{01/02}$	TE_{02}	0.23	37	CW
		70	$TE_{01/02}$	TE_{02}	0.21	36	3
		84	$TE_{15,2}$	$TE_{15,2/4}$	0.5	33	0.1

Table I: Performance parameters of gyrotron oscillators for electron cyclotron resonance heating (ECRH) (28-84 GHz) and lower hybrid heating (8 GHz) of plasmas in magnetic confinement fusion studies.

Institution	Frequency [GHz]	Mode cavity	Mode output	Power [MW]	Efficiency [%]	Pulse length [s]
KfK, PHILIPS, [24]	140	TE_{03}	TE_{03}	0.12	23	0.4
KfK, Karlsruhe [24]	132.6	$TE_{9,4}$	$TE_{9,4}$	0.42	21	0.005
	140	$TE_{10,4}$	$TE_{10,4}$	0.69	27	0.005
	147.4	$TE_{11,4}$	$TE_{11,4}$	0.3	17	0.005
MITSUBISHI,	120	$TE_{02/03}$	TE_{03}	0.16	25	0.06
Amagasaki [25]	120.3	$TE_{15,2}$	$TE_{15,2}$	0.61	30.6	0.0001
SALUT, IAP,	110	$TE_{15,4}$	TEM_{00}	0.5	33	0.5
Nizhny Novgorod [9,10]	140	$TE_{22,6}$	TEM_{00}	0.9	36	0.4
				0.5	33	2.0
	167		TEM_{00}	0.9	30	0.3
				0.5	30	0.7
THOMSON, Velizy [20]	100	TE_{34}	TE_{34}	0.19	30	0.07
	110	TE_{93}	TE_{93}	0.42	17.5	0.002
		TE_{64}	TE_{64}	0.27	16	0.05
TOSHIBA,	110	$TE_{22,2}$	TEM_{00}	0.37	22	0.3
Shimoishigami [25,26]				0.55	22	0.002
	120	TE_{03}	TE_{03}	0.15	30	0.01
	120	$TE_{12,2}$	TEM_{00}	0.55	30	0.1
				0.25	30	0.2
TORIY, IAP, Moscow,	140	$TE_{22,5}$	TEM_{00}	0.97	34	0.3
Nizhny Novgorod [10,27,29]				0.58	34	2.0
VARIAN,	106.4 ($2\Omega_c$)	$TE_{02/03}$	TE_{03}	0.135	21	0.1
Palo Alto [2,22]	106.4	$TE_{12,2}$	$TE_{12,2}$	0.4	30	0.1
	110	$TE_{15,2}$	$TE_{15,2}$	0.5	28	1.0
				0.3	28	2.0
		$TE_{22,2}$	$TE_{22,2/4}$	0.5	27	2.5
	140	$TE_{02/03}$	TE_{03}	0.1	27	CW
	140	$TE_{15,2}$	$TE_{15,2}$	0.26	28	5.0
				0.32	30	3.5
				1.04	38	0.0005

Table II: Present development status of high frequency gyrotron oscillators for ECRH and stability control in magnetic fusion devices (f $\geq$ 100 GHz, $\tau \geq$ 1 ms).

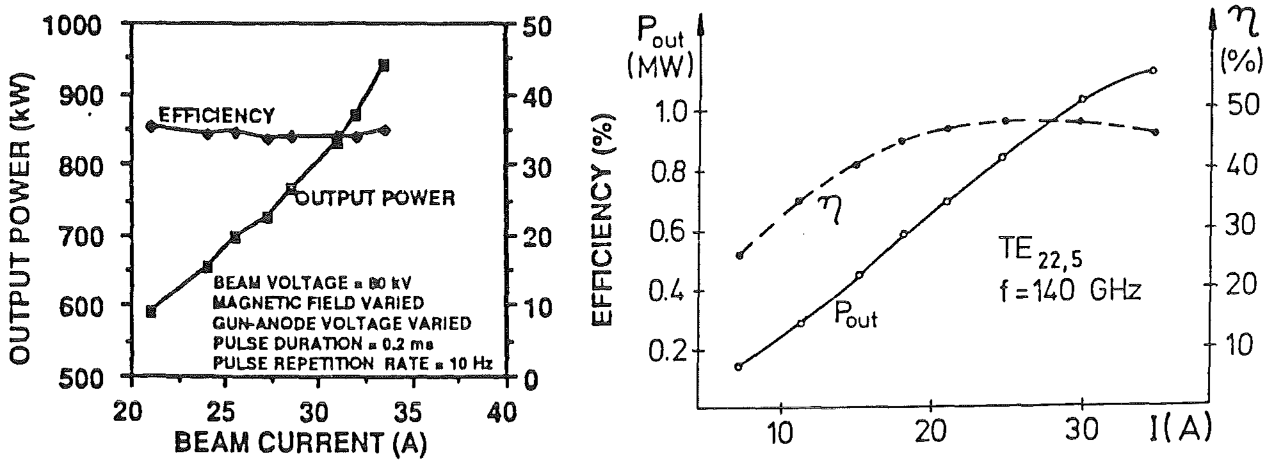

Fig. 9 Output power and efficiency versus beam current of 140 GHz gyrotrons, left: VARIAN [2], right: IAP [29].

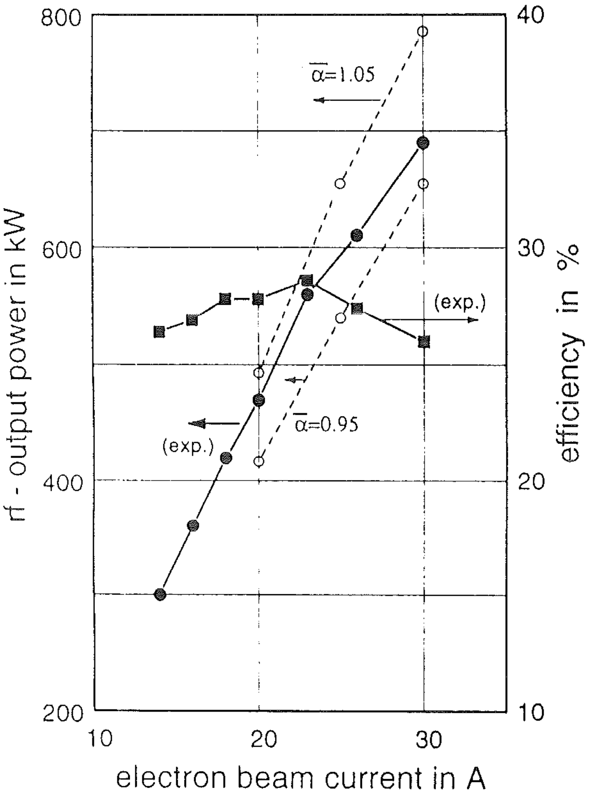

Fig. 10
Output power and efficiency of the KfK 140 GHz $TE_{10,4}$ mode gyrotron as a function of beam current,
beam voltage = 87 kV
gun anode voltage = 23 kV
magnetic field = 5.5 T.
The dashed lines correspond to numerical simulations with an average velocity ratio of 0.95 and 1.05.

With increasing operating frequency, power level and pulse duration a number of problems arise which necessitate significant changes in the gyrotron design approach. The main difficulties encountered in the realization of efficient megawatt CW mm-wave gyrotrons are connected with:

- formation of an electron beam with sufficient orbital energy ($\alpha \geq 1.5$) and small velocity spread (electron gun design).
- propagation of the electron beam, spurious oscillations in the beam tunnel between the electron gun and the interaction cavity (see Fig. 1), voltage depression (dependent on R_e/R_o, where R_e is the electron beam radius), space charge effects and beam instabilities.
- ohmic wall losses in the cavity (cavity heating).
- mode selectivity in a highly overmoded cavity, single mode operation, good mode separation of working mode from competing modes.
- unwanted mode conversion in the electrodynamic system of the tube.
- thermal loading of the electron beam collector.
- heating of the output window, selection of output mode.
- enhancement of efficiency up to 50-60%.

Design trade-offs and operating limits will be necessary.

Electron Gun. The electron guns employed in gyrotrons provide a hollow beam of spiraling electrons which have a large fraction of their energy in velocity components transverse to the tube axis. Magnetron injection guns (MIG) have thus far been used most successfully with their cathodes operated in a temperature limited mode. The main factors producing the velocity spread are [10]: spread of the initial velocities, roughness of the emitting surface, disturbance of axial symmetry of the electron gun, space charge effects within the beam, inhomogeneous fields on the cathode and nonadiabatic fields in the intermediate region (compression zone) between the cathode and the interaction cavity. Relatively high compression ratios of up to 30-40 are used [24]. Diode-type guns [10] as well as triode-type guns with a modulation anode [2], which give the option of powerless modulation of the electron beam and thus of the output power for heat pulse propagation experiments [24] are employed.

Beam Compression Region. The beam downtaper (beam tunnel) which reduces the wall radius from the electron gun to the interaction cavity has to be heavily loaded with specifically shaped rings of lossy dielectrics to suppress spurious oscillations [2].

Interaction Cavity. The choice of the working mode of a high-power CW mm-wave gyrotron is based on an intricate set of design trade-offs. The first 140 GHz gyrotrons [2, 24] employed rotationally symmetric TE_{03} mode cavities. The TE_{0n} circular symmetric family of modes is part of a general class of modes called volume modes. Most of the stored energy in a volume mode resides in the central region of the cavity. As a result, for optimum coupling, the electron beam is placed on an inner maximum of the resonator electric field. Consequently the beam radius is relatively small compared with the size of the cavity.

For frequencies above 100 GHz and power levels approaching 1 MW, ohmic losses in the cavity walls necessitate the use of larger higher order mode cavities. If the electron beam remains located on one of the inner maxima, potential depression quickly limits the amount of beam current that may be passed through the resonator for a given beam voltage and pitch factor α. In addition, the problem concerning mode competition with the neighbouring TE_{2n} mode becomes more severe. With increasing n, frequency spacing between the TE_{0n} and TE_{2n} modes decreases. If the electron beam is placed on one of the outer maxima the cavity Q has to be increased to keep the efficiency high enough, thereby nullifying much of the ohmic loss reduction realized in using a higher order cavity.

To alleviate the many conflicting requirements posed on cavity wall losses, potential depression, mode competition and efficiency considerations, a different interaction approach has to be utilized. Only rotating whispering gallery modes (WGM: TE_{mn} with $m >> 1$ and $n = 1,2$) or asymmetric volume modes (AVM: TE_{mn} with $m >> 1$ and $n > 2$) are now considered to have the potential to meet high power requirements (0.5-1.0 MW) in CW operation at frequencies around 140 GHz [1,2,7-10,20-29].

A general scaling law for the maximum power density P_Ω in the cavity walls is approximately given by [2,24]:

$$P_\Omega = K \, P_{out} \, Q \, f^{5/2} \, / \, (X_{mn}'^{2} - m^2) \tag{7}$$

when P_{out} is the power output and K is a scaling constant which depends upon a number of factors including material selection, surface finish, manufacturing process, operating temperature and thermal cycling history of the cavity.

Typical limits for P_Ω given in literature are about 3 kW/cm^2 (without extending to exotic cooling techniques) leading with $Q \cong 700\text{-}1000$ to working modes satisfying

$$X'^2_{mn} - m^2 \geq \begin{array}{l} 500 \text{ for } P_{out} = 0.5 \text{ MW} \\ 1000 \text{ for } P_{out} = 1.0 \text{ MW} \end{array} \quad (8)$$

In an oversized electrodynamic system the mode spectrum is very dense; therefore the cyclotron resonance condition (see the dispersion diagram Fig. 3) can be fulfilled for the operating mode and several neighbouring modes simultaneously. Mode competition may result in unstable oscillations, efficiency reduction and complete quenching of the operating mode oscillations. Usually, to provide mode selection one tries to diminish the Q factors and the coupling impedances of the parasitic modes with the electron beam. The coupling of the desired working mode with beam electrons is strongest if the nominal beam radius in the resonator coincides with the inner electric field maximum (approx. caustic radius of the mode) as shown in Fig. 11 for the $TE_{10,4}$ mode of the KfK gyrotron [24]. In order to avoid problems with beam voltage depression and possible beam instabilities a ratio $R_e/R_o \geq 0.45$ is required.

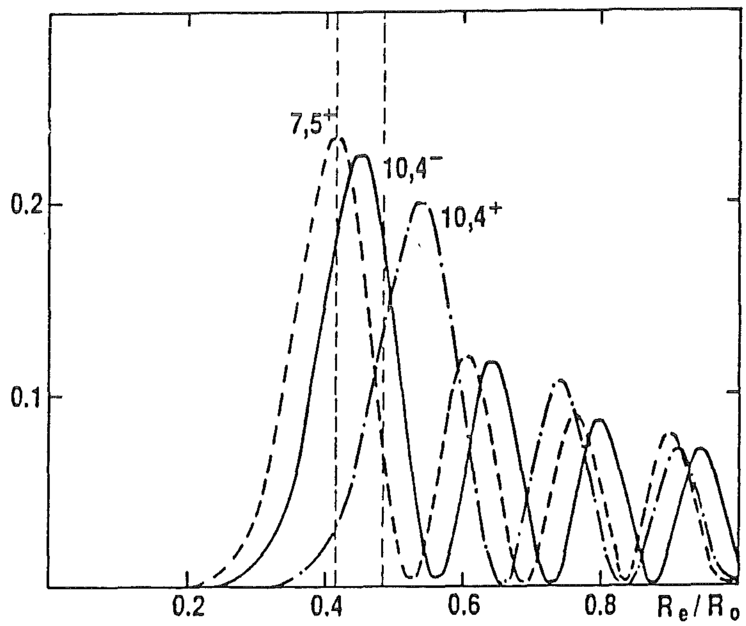

Fig. 11. Coupling coefficients vs normalized radius for the $TE_{10,4}$ ± and $TE_{7,5}$+ modes. The vertical lines delineate the beam position (a beam of thickness $4r_L$ is assumed to be centered at $R_e = 3.65$ mm for $R_0 = 8.11$ mm)

Up to now, stable single mode oscillations have been obtained for AVMs in simple cavities having a diameter of up to 23 λ [1,36]. Higher efficiencies and more stable operation can be achieved if the working mode is chosen to be as isolated as possible from possible competing modes. Since there will be many modes close in frequency to the candidate mode, one searches for modes such that nearby possible competitors couple only weakly to the beam.

This requires also good beam quality and careful choice of beam radius. For a first overview the starting current relation for candidate (c) and parasitic (p) mode and the frequency separation can be considered. Good candidates satisfy the criterion that $I_p/I_c > R$ when $|\Delta f|/f = |1 - f_p/f_c| < \varepsilon$ with R and ε as large as possible [24]. TE_{mn} modes with $m \geq 20$ and n = 4-6 are promising candidates for megawatt 140 GHz gyrotrons [9,24,27,28]. At the upper limit $D/\lambda \approx 20$ the experimental efficiency of approximately 25 % could be improved to 35 % by taking additional mode selection measures utilizing a coaxial cavity [29] (see Fig. 12). Introduction of an inner rod conductor into the cylindrical resonator lowers the voltage depression (higher efficiency) and permits one to affect the Q factor of modes with high radial indices n whose fields are disturbed by this rod. Improved mode selection and high efficiency may also be achieved using coupled (complex) cavities [29] (see Fig. 12) or two section cavities with a prebunching cutoff waveguide section [31].

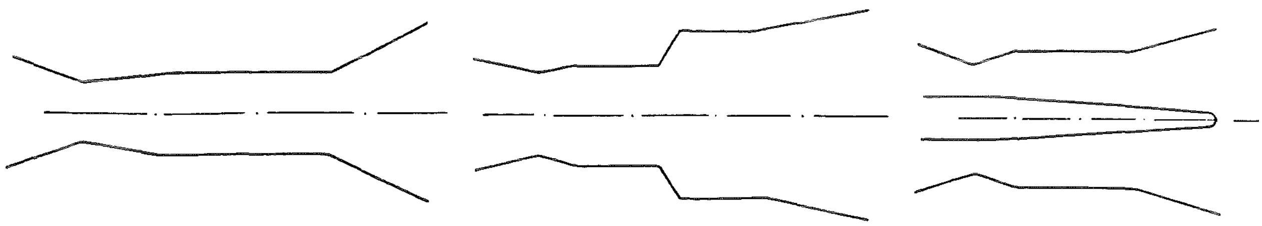

Fig. 12 Profile of conventional cylindrical resonator (left), two section-coupled resonator (middle) and coaxial resonator (right).

Slow frequency step tuning by variation of the magnetic field and corresponding change of the operating mode (series of $TE_{m,n}$ modes with n=const) has been demonstrated experimentally [8,9] (see Fig. 13). Recent computational studies performed at KfK [32] show that fast frequency tunability may be feasible by simultaneously changing beam and modulation anode voltage.

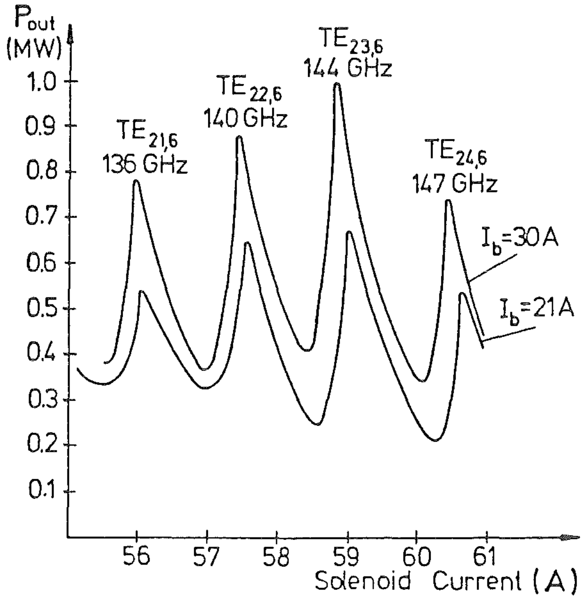

Fig. 13 Output power versus magnetic field of IAP-SALUT 140 GHz gyrotron [9,29].

Output Taper, Electron Beam Collector and Output Coupler. CW gyrotron oscillators having the classic configuration as indicated in Fig. 1 employ standard output coupling where the electron beam collector also serves as the output waveguide. A nonlinear uptaper links the interaction cavity to the large diameter collector and in high power long pulse tubes, a nonlinear downtaper is incorporated between the collector and the output window waveguide. The entire uptaper/collector/downtaper combination is designed to preserve the purity of the mode generated in the cavity [2]. Usually a series of small magnet coils is employed along the length of the collector to aid in spreading the spent electron beam uniformly over a sufficiently large area to avoid heat load limits or electrical breakdown in the collector. Mode purity requirements preclude the option of very large diameter collectors. For 1 MW, CW tubes the implementation of an output coupling approach that separates the spent electron beam from the outgoing RF power is required. Such a configuration additionally allows the use of a depressed collector to improve the overall system efficiency and leads to a reduction of the overall height of the tube.

Two possible scenarios are currently being considered in addressing this problem. The first allows for the radial extraction of the electron beam through a slot in the output waveguide, while the generated mm-wave power continues straight through the tube as in the classic design employed in most previous gyrotrons (cavity mode is also the output mode)[2].

The second method of separating the electron beam from the mm-wave output provides the radial extraction of the microwave power while the electron beam continues straight through to a large diameter collector. This approach has been successfully used in Russian gyrotrons [1,9, 10, 27, 29] with the incorporation of a quasi-optical coupler. This type of coupler transforms the rotating cavity output mode into a linearly polarized Gaussian beam. A schematic of a gyrotron with built in quasi-optical mode transducing antenna, utilizing two mirrors, is shown in Fig. 14 [24]. Advanced quasi-optical couplers provide conversion efficiencies close to 98% [29, 30]. This second solution has a number of advantages:

- the Gaussian mm-wave beam is lateral and ready for propagation [6].
- the output power reduction due to the so-called long-line effect (window- or load reflections seen by the cavity) is minimized since the quasi-optical mode transducer works as an isolator; thus mode competition becomes less critical.
- beam sweep collectors with optimized surface can be used [29]. The collector profile guarantees that the time averaged electron beam deposition is uniform.

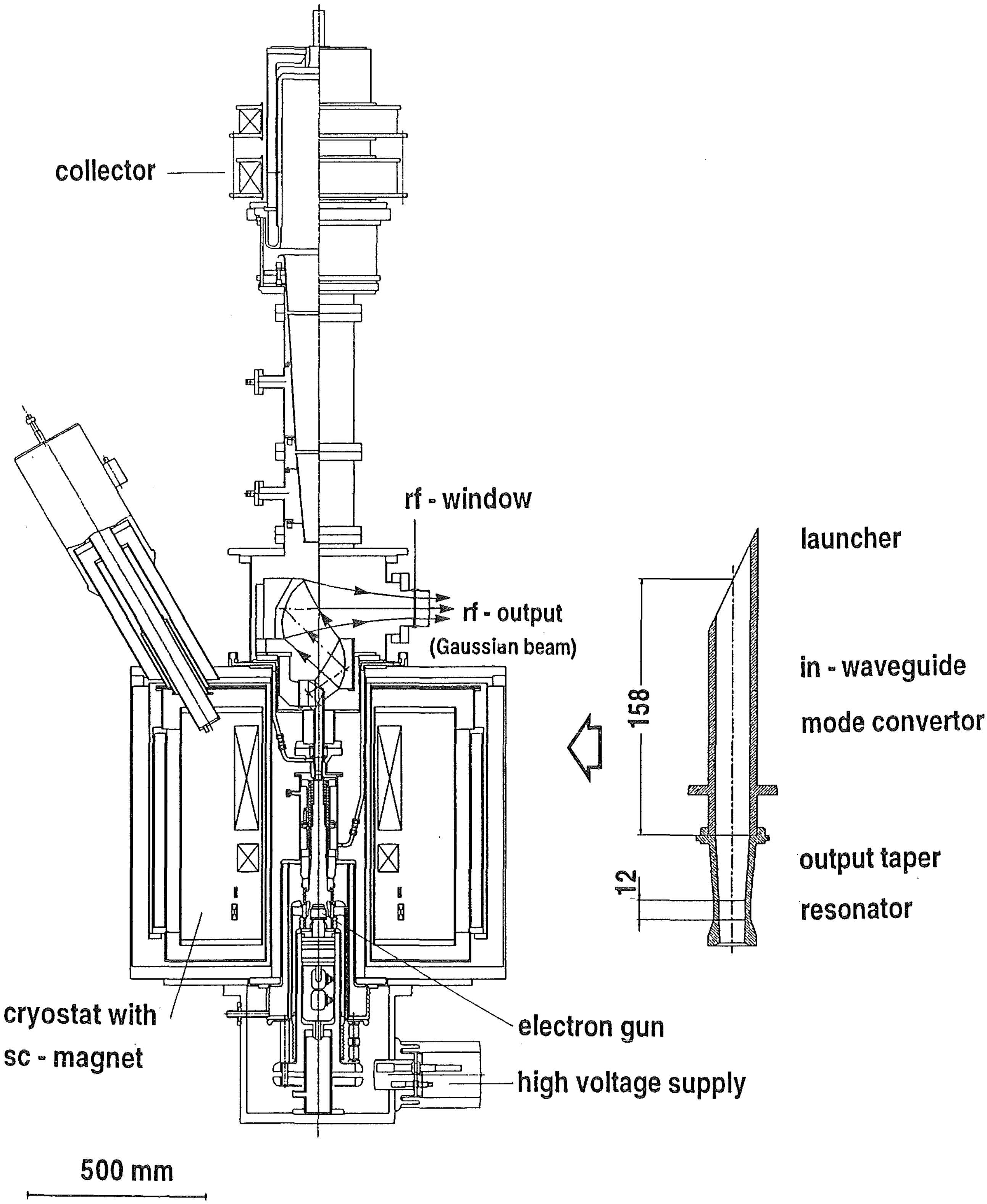

Fig. 14 Schematic layout of an advanced asymmetric volume mode (AVM) gyrotron with quasi-optical converter [24].

Output window. In the case of monochromatic radiation, wave reflection from the window is usually eliminated by one of two methods: (a) a single periphery-cooled disk is used having a thickness of a multiple of half the wavelength in the dielectric and (b) two of such resonant disks are combined to a double disk window (with surface cooling) in which the distance between the disks is tunable. Present day long-pulse high power gyrotrons (Table II) either employ FC-75 face cooled double disk Al_2O_3 ceramic or sapphire windows [2,24] or ballistic, water edge cooled, single disk boron nitride windows [9,27,29]. However, such solutions are not able to carry 1 MW, CW at mm-wavelengths. In any design that is capable of transmitting such power levels the major limitations stem from the combination of thermal and mechanical stresses. This environment requires strong, low-loss window materials and optimized mechanical designs. The possibility of using a cryogenically-cooled, single-disk, sapphire window looks attractive [2, 24]. This is due to the significantly lower RF loss and higher heat conductivity of sapphire at these temperatures. Operation at LN_2 temperature (liquid nitrogen at $\cong$ 80 K) is possible if losses are sufficiently low. Solutions using liquid neon, gaseous helium or even liquid He are also under consideration.

As a potentially new material for noncryogenically cooled gyrotron windows, chemical-vapor-deposition (CVD) diamond is attractive due to its phenomenal tensile strength, modest dielectric constant, low loss and high thermal conductivity. However, present day CVD capabilities have not yielded sufficiently thick samples with the required window diameter.

If frequency tuning is needed, the window should be intrinsically broadband. A possible solution is an improved "moth-eye" configuration [33, 34] with disks having grooves with optimized shape instead of pyramidal corrugations. Multi-layer windows (variation of permittivity) or Brewster angle windows are other possibilities.

5 Very high frequency gyrotron oscillators

The development of high power gyrotrons for the short millimeter- and submillimeter-wave region is important for applications such as ECRH of high-field tokamak experiments with confining magnetic field $B_o \geq$ 10T [35,36], for active plasma diagnostics such as mm-wave scattering to determine velocity distributions of ions and to study drift instabilities [10], and for radar and spectroscopy [16]. During the past several years excellent results have been obtained with pulsed and CW gyrotrons designed for operation at the second harmonic (s=2) of the electron cyclotron frequency employing superconducting [9,37-39] or Bitter magnets [40]. The most impressive recent results are given in Table III. The 3 dB frequency line width (FWHM) of gyrotron radiation was measured to be around $\leq$ 200 kHz [10, 40, 41]. A high spectral purity: ratio of noise power to total rf power $P_N/P_o < 10^{-18}$/Hz, has been verified [22].

Institution	Frequency [GHz]	Mode	Power [kW]	Efficiency [%]	Pulse length [ms]
IAP, N.Novgorod [10,37]	157	TE_{03}	2.4	9.5	CW
	250	TE_{02}	4.3	18	CW
	250	TE_{65}	1	5	CW
	326	TE_{23}	1.5	6	CW
MIT, Cambridge [36,40]	209	TE_{92}	15	3.5	0.001
	241	$TE_{11,2}$	25	6.5	0.001
	302	TE_{34}	4	1.5	0.0015
	339	$TE_{10,2}$	4	3	0.0015
	363	$TE_{11,2}$	7	2.5	0.0015
	417	$TE_{10,3}$	15	6	0.0015
	457	$TE_{15,2}$	7	2	0.0015
	467	$TE_{12,3}$	22	3.5	0.0015
	503	$TE_{17,2}$	10	5.5	0.0015
UNIVERSITY, Fukui [38]	383	TE_{26}	3	3.7	1
	402	TE_{55}	2	3	1

Table III Capabilities and performance parameters of mm- and submillimeter-wave gyrotrons operating at the second harmonic of the electron cyclotron frequency, with output power $\geq$ 1 kW.

Institution	Frequency [GHz]	Mode	Power [MW]	Efficiency [%]	Pulse length [μs]
MIT, Cambridge [8,35,36]	140	$TE_{15,2}$	1.33	40	3
	148	$TE_{16,2}$	1.3	39	3
	188	$TE_{18,3}$	0.6		3
	↓	↓	↓		↓
	225	$TE_{23,3}$	0.37		3
	231	$TE_{38,5}$	1.2	20	3
	236	$TE_{21,4}$	0.4		3
	↓	↓	↓		↓
	287	$TE_{28,4}$	0.2		3
	280	$TE_{25,13}$	0.78	17	3
	267	$TE_{22,5}$	0.537	19	3
	↓	↓	↓		↓
	320	$TE_{29,5}$	0.4	20	3
	327	$TE_{27,6}$	0.375		3
IAP,	250	$TE_{20,2}$	0.3	31	30 - 80
Nizhny Novgorod [10]	350		0.13	17	30 - 80
	430		0.08	10	30 - 80
	500		0.1	8.2	30 - 80
	540		0.06	6	30 - 80
	650		0.04	4	40

Table IVa Capabilities and performance parameters of pulsed millimeter- and submillimeter-wave gyrotron oscillators operating at the fundamental electron cyclotron resonance.

Institution	Frequency [GHz]	Mode	Power [MW]	Efficiency [%]
MIT, Cambridge [36]	187.7	$TE_{32,4}$	0.65	12
	201.6	$TE_{35,4}$	0.92	18
	209.5	$TE_{33,5}$	0.54	15
	213.9	$TE_{34,5}$	0.89	18
	218.4	$TE_{35,5}$	0.56	14
	224.3	$TE_{33,6}$	0.90	17
	228.8	$TE_{34,6}$	0.97	18
	265.7	$TE_{39,7}$	0.64	12
	283.7	$TE_{43,7}$	0.33	10
	291.6	$TE_{41,8}$	0.887	18

Table IVb Step tuning of MIT gyrotron oscillator (with large MIG [36]) operating at the fundamental electron cyclotron resonance (pulse length 1.5 μs).

Fundamental cyclotron resonance interaction has been studied using a special pulsed high field solenoid for B_0=14-27 T [10] or a Bitter magnet rebuilt to operate at up to B_0=14 T [35,36]. Key issues to be addressed are: stability of electron beams with compression ratio $\geq$ 40, mode competition in cavities with $D/\lambda \geq 20$ and improved cavity design, and step-tuning of frequency up to 327 GHz. Tables IVa and IVb summarize the present capabilities and performance parameters of such gyrotrons. Operating at both fundamental and the 2nd harmonic of the electron cyclotron frequency enables the gyrotron to act as a medium power (several 100 W), step tunable, mm- and sub-mm wave source in the frequency range from 150 to 640 GHz [38].

6 Gyrotrons for technological applications

The use of gyrotron oscillators for technological applications as material processing and plasma chemistry [11] appears to be of great interest if relatively simple, low cost devices are realized which are easy in service such as magnetrons. In CW gyrotrons with medium output power from 10 to 30 kW relatively low operating modes can be used even in the mm-wave range. Reliability, efficiency, feasibility and simplicity are the main problems instead of the thermal load and mode selectivity problems of ECRH gyrotrons. Devices with low magnetic field (normal conducting magnet), low anode voltage, high efficiency and simple output coupling are under development. The state of the art in this area is summarized in Table V.

Institution	Frequency [GHz]	Mode cavity	Mode output	Power [kW]	Efficiency [%]	Voltage [kV]
SALUT, IAP,	15	TE_{01}	TE_{01}	4	50	15
Nizhny Novgorod,	30 ($2\Omega_c$)	TE_{02}	TE_{02}	20	30	20
TORIY, Moscow	37.5		TEM_{00}	20	30	40
[9,11,27,29]	78	TE_{32}	TE_{11}	10	30	30
	82	$TE_{11,3}$	TEM_{00}	30	30	40
	160 ($2\Omega_c$)	TE_{03}	TE_{03}	2.4	9.5	18
VARIAN, Palo Alto [2]	28	TE_{02}	TE_{02}	15	40	40

Table V Performance parameters of present CW gyrotron oscillators for technological applications.

7 Quasi-optical gyrotrons

Although most gyrotron research has been based on the cylindrical waveguide cavity, results have also been obtained with a quasi-optical cavity [7, 42]. The quasi-optical gyrotron is a gyro-device in which the interaction between the electromagnetic wave and the electron beam occurs in a Fabry-Perot type resonator placed transversely to the static magnetic field (Fig. 2). Operation in the mm-wave range of frequency and at megawatt power level is possible since the ohmic heat load on the mirror surfaces can be kept within the usual limits of 1-3 kW/cm^2 by adjusting the resonator parameters. The operating mode is a high order Gaussian TEM_{00q} (with longitudinal mode index $q>200$) so that the frequency can be tuned over a wide range by variation of the mirror distance (change of q). The separation between the spent electron beam and the microwave allows easy implementation of a depressed collector in order to increase the overall system efficiency.

The state-of-the-art of quasi-optical gyrotrons is summarized in Table VI. The two key issues of the current research are: The output coupling scheme and efficiency enhancement. Concerning the issue of a Gaussian output coupling scheme, the use of a grating mirror appears to be the best approach, as confirmed by hot test experiments where up to 99% of the power was coupled into a HE_{11} waveguide [43]. Three methods are being considered for efficiency enhancement [7,42]:

- the use of a sheet electron beam instead of the hollow MIG beam of conventional gyrotrons. Issues of sheet beam stability must still be investigated.
- the use of a depressed collector.
- the quasi-optical gyroklystron configuration. In this case the main difficulties lie in the necessity of amplitude and phase control by a feedback loop between the energy extracting resonator and the prebuncher. Mode priming and α-priming are being studied.

Institution		Frequency [GHz]	Mode resonator	Power [kW]	Efficiency [%]	Pulse length [ms]
ABB, Baden	[18]	92	TEM_{00q}	90	10	10
CRPP, Lausanne	[7]	100	TEM_{00q}	90	12	15
NRL, Washington D.C.	[42]	115	TEM_{00q}	600	9	0.015
				220	15.4	0.015
				73	20.0	0.015

Table VI Present development status of quasi-optical gyrotron oscillators.

8 Cyclotron autoresonance masers (CARMs)

CARM oscillators and amplifiers are presently only at the stage of proof of principle experiments but recent experimental successes show their intrinsic potentialities. The status of CARM performance parameters is summarized in Table VII. The key issues for the future development of such devices are:

- Very high electron beam quality is required to obtain a high efficiency. The efficiency drops for $\Delta v_z/v_z \geq 2\%$ from 40% to 20%. Recently, an efficiency of 10% has been achieved in 36 and 50 GHz, TE_{11} CARM oscillators employing an improved Bragg resonator [44]. By keeping the interaction region short (less than 10 cyclotron orbits), the effect of velocity spread is reduced. The interaction efficiency is found to be substantially increased when the axial magnetic field is tapered.
- High energy electron beam transport with low interception in the body.
- The competition between other interaction processes such as the gyrotron or the backward wave instabilities. These unwanted oscillations can be suppressed by choosing an optimum bunching parameter [44,45].

Institution	Frequency [GHz]	Mode	Power [MW]	Efficiency [%]	Gain [dB]	B-Field [T]	Voltage [MV]	Current [kA]	Type
IAP	35.7	TE_{51}	25	10	-	1.3	0.5	0.5	oscil.
IAP, IHCE	37.5	TE_{11}	10	4	30	0.5	0.5	0.5	ampl.
IAP,IHCE,JINR	50	TE_{11}	30	10	-	0.7	1.0	0.3	oscil.
IAP	66.7	TE_{21}	15	3	-	0.6	0.5	1.0	oscil.
IAP,IHCE,JINR	68	TE_{11}	50	8	-	1.0	1.2	0.5	oscil.
IAP	69.8	TE_{11}	6	4	-	0.6	0.35	0.4	oscil.
IAP [44]	125	TE_{41}	10	2	-	0.9	0.5	1.0	oscil.
MIT Cambridge	27.8	TE_{11}	1.9	5.3	-	0.6	0.45	0.080	oscil.
[45]	30	TE_{11}	0.1	3	-	0.64	0.3	0.012	oscil.
	32	TE_{11}	0.11	2.3	-	0.63	0.32	0.015	oscil.
	35	TE_{11}	10	3	45	0.7	1.5	0.25	ampl.
UNIV. Michigan [46]	15	TE_{11}	7	1.5	-	0.45	0.4	1.2	oscil.
LLNL Livermore [47]	220	TE_{11}	50	2.5	-	3.0	2.0	1.0	oscil.

IAP Nizhny Novgorod, IHCE Tomsk, JINR Dubna

Table VII State-of-the-art of CARM experiments (short pulse)

9 Gyroklystrons, gyro-TWTs, gyro-BWOs and other gyro-devices

As in the cases of gyromonotron and CARM, the efficiencies of gyroklystrons, gyro-TWTs and gyro-BWOs strongly depend on beam quality. The longer interaction time in amplifiers allows the phase bunching of the electrons to be more degraded by velocity spread. Efficiency may be improved by keeping the gain per unit length high, and thus for a given overall gain, making the interaction region as short as possible [48-58]. Improved electron guns (e.g. Pierce guns with kickers) are under development [44,59]. Electron beams with relatively low α (α = 0.8) have resulted in stable saturated gyro-TWT operation at broad bandwidth at the expense of lower efficiency [50]. Dramatic improvement in performance appears to be achievable by tapering of both the magnetic field (ramped field) and the wall radius along the axis of the interaction region to maintain the resonance condition over a wide frequency range [50,51]. This precise axial contouring is a topic of intensive current study. The gyro-TWT is potentially capable of much larger bandwidth than the gyroklystron. Key issues for gyroklystrons are stray oscillations in the drift regions between the different cavities, magnetic field profiling and penultimate tuning [3, 52-56]. Tables VIII to X summarize the actual experimental parameters of gyroklystrons, gyro-TWTs and gyro-BWOs, respectively. The duty factors of the gyroklystrons developed by VARIAN (Palo Alto), TORIY (Moscow) and IAP (Nizhny Novgorod) are 5 % (with 0.2 % bandwidth), 1 % (with 1.5 % bandwidth) and 0.05 % (with 0.5 % bandwidth), respectively. In the CW regime a peak output power of 2.5 kW at an efficiency of 25 % (beam voltage 22 kV, beam current 0.46 A) has been achieved in Russia (TORIY Moscow in collaboration with IAP Nizhny Novgorod). The measured large-signal gain of this gyroklystron is 30 dB and the experimental half-power bandwidth is 0.35 %. Rapid improvement in performance of gyro-amplifiers is expected in the near future since the development of those devices is in a considerably more preliminary state than the development of gyromonotrons.

Institution	Frequency [GHz]	Mode	No. of cavities	Power [MW]	Efficiency [%]	Gain [dB]	
NRL, Washington D.C.	4.5	TE_{10}	3	0.07	40	36	
[16,36,48,49]	85	TE_{13}	2	0.05		20	
	85	TEM_{00}	2	0.1	30	18	q.o. with depressed coll.
UNIV. MARYLAND	10	TE_{01}	2	24	30	34	
[52-54]	10	TE_{01}	3	27	32	37	max. power
			3	16	37	33	max. efficiency
			3	20	28	50	max. gain
	19.8	$TE_{01}/TE_{02}(2\Omega_c)$	2	32	28	27	
IAP Nizhny Novgorod	15.8	TE_{02}	3	0.16	39	30	max. efficiency
TORIY, Moscow [55,56]	35	TE_{02}	2	0.75	25	20	max. power
			2	0.35	32	19	max. efficiency
	35	TE_{01}	4	0.16	48	42	
			3	0.30	40	40	
IAP Nizhny Novgorod [56]	93.2	TE_{01}	4	0.065	26	33	max. power
			4	0.057	34	33	max. efficiency
VARIAN, Palo Alto [16]	28	$TE_{01/02}$	2	0.076	9	41	

Table VIII Gyroklystron experimental results (short pulse, bandwidth $\leq$ 2 %).

Institution	Frequency [GHz]	Mode	Power [kW]	Efficiency [%]	Gain [dB]	Bandwidth [%]	
UC LOS ANGELES [71]	10	TE_{10}	55	11	27	11	diel.coat.w.g.
UNIV. HSINCHU [50]	35.8	TE_{11}	18.4	18.6	18	10	
NRL, Washington D.C.	32.5	TE_{10}	5	10	16.7	33	
[16,51]	34.3	TE_{01}	16.6	7.8	20	1.4	
VARIAN, Palo Alto[16]	5.18	TE_{11}	120	26	20	7.3	
	95	TE_{11}	15	6.3	30	1.6	

Table IX Present development status of gyro-TWTs (short pulse).

Institution	Frequency [GHz]	Mode	Power [kW]	Efficiency [%]	Bandwidth [%]	
NRL, Washington D.C. [57]	29.2	TE_{10}	6	15	3	electric tuning
					13	magnetic tuning
UNIV. HSINCHU [58]	34	TE_{11}	20-67	6.5-21.7	5	
MIT.LLNL Livermore [59]	138	TE_{12}	1	0.5	6.5	

Table X First experimental results on gyro-BWOs (short pulse).

So far, we have considered gyro-devices driven by the kinetic energy stored in the small-orbit Larmor gyration of electrons in a magnetic field. By contrast, in the large-orbit gyrotron (also known as a gyromagnetron or cusptron [16]), a beam of electrons is passed through a magnetic cusp so that the beam goes into a fast rotational mode in which all of the electrons have axis-encircling orbits. This large-orbit beam then interacts downstream in a cavity with a magnetic field to produce microwaves. Although not as efficient as conventional gyrotrons operating at the fundamental, large-orbit gyrotrons have demonstrated an ability to run at very high multiples (e.g., 10 to 20) of the cyclotron frequency. The magnicon, an enhancement of the original gyrocon [16] and finally the peniotron are other large-orbit devices.

The peniotron is based on an interaction first described by Ono and his coworkers in 1962 [73], shortly after the discovery of the ECM. The peniotron mechanism, however, is very different from the ECM interaction in two respects. First, it operates in a mode with azimuthal index m, which must be related to the cyclotron harmonic index s by

$$m = s + 1 \quad ; \quad \text{i.e. } \omega = (m - 1)\,\Omega + k_z v_z \tag{9}$$

Second the interaction extracts roughly the same amount of energy from each electron, regardless of its phase, so that there is no bunching [74]. As a consequence, the efficiencies predicted by ideal theories are quite high, higher than in ECMs, where bunching occurs and a minority of the electrons actually draw energy from the fields. High efficiencies at cyclotron harmonics are also possible. Selection of modes with large azimuthal wavenumbers at high cyclotron harmonics is accomplished with a magnetron-like structure in the cavity, as in a large-orbit gyrotron. Effective coupling of the beam and fields is effected by using beams placed close to the wall with axis-encircling orbits. Computer simulations indicate that the efficiency is rather insensitive to spreads in the guiding center locations for the beam electrons, but that beam loss to the nearby wall is a limiting factor [74].

10 Free electron masers (FEMs)

10.1 Potentialities

The FEM (Free Electron Maser) appears potentially capable of fulfilling all the requirements for a frequency agile high power mm-wave source. Coverage of the entire frequency range of 130-260 GHz presents no severe problems, and even higher frequencies are quite feasible. Rapid tunability over more than $\pm$ 5 % could be obtained by variation of the beam energy. The interaction occurs in a cavity operating in low-order modes, which have very good coupling to a Gaussian beam output. The relatively low RF wall loading and the use of high electron beam energy (>0.5 MeV) are compatible with a high unit power if the electron beam interception could be maintained at an acceptable level. A survey of FEM development status (experiments) is presented in Table XI.

10.2 Accelerator options and key issues

In principle, for the mm-wave range, the FEM could be powered by either an induction LINAC, and RF LINAC with beam energy at 3 - 10 MeV, or an electrostatic accelerator at 0.5-3 MeV. One of the problems of the induction LINAC is the large size and complexity of the device. Another difficulty is the very high peak power at low repetition rate and, therefore, the possible impact of non-linear effects associated with pulsed output at GW peak power. The RF-LINAC is also a pulsed device with a peak power up to 50 MW; this is deemed to be acceptable for ECW interaction in the linear regime. Development of a source having an average output of 1 MW should be possible using proven technology. An oscillator with a high system efficiency requires a sophisticated recirculation and recovery scheme. A FEM amplifier with a tapered undulator has already achieved a high extraction efficiency per pass (40 %) without energy recovery. The electrostatic accelerator allows true CW operation and has the potential of achieving efficiencies in the 50 % range through energy recovery (but very good beam quality is required).

Key issues common for both accelerator options are:

- the design of the output coupling scheme,
- the implementation of techniques to suppress the side-band instability.
  Both problems may be solved using a special interaction circuit employing a stepped rectangular HE_{11} waveguide together with phased plane 100 % reflectors [72].

The electrostatic accelerator would also require:

- development for the transport of a multiampere beam at energies around or larger than 1 MeV at extremely low (<0.5 %) body current on the undulator channel.
- development of a short-period undulator (period below 2 cm) at frequencies larger than 260 GHz.

The specific important issue for RF LINAC is:

- an efficient energy recovery system (the system efficiency is a sensitive function of the "recovery" efficiency: 96 % (resp. 89 %) is necessary to obtain 20 % (resp. 10 %) system efficiency.

Institution	Frequency [GHz]	B_w [T]	λ_w [mm]	Mode	Power [MW]	Efficiency [%]	Gain [dB]	Voltage [MV]	Current [kA]	Accelerator	Pulse-Length [μs]	Type
ENEA Frascati [60,61]	85-200	0.63	25	TE_{01}□	0.0015	$1.6\cdot10^{-4}$		2.3	0.004	Microtron	0.18	oscillator
EP Palaiseau [62]	120	0.03	20	TE_{11}○	11.5	6.4		0.6	0.3	Electrostatic	0.02	superrad.
FOM Rijnhuizen [63]	≥ 2700	0.04	65		0.0001	$2\cdot10^{-8}$	20	25	0.0002	RF LINAC	0.03	amplifier
ILE Osaka [64]	250				0.6			4	0.5	Ind. LINAC		
JAERI, Ibaraki [65]	45	0.18	45	TE_{11}○	6	2	52	1.0	0.3	Ind. LINAC	0.08	amplifier
LLNL, Livermore [14,15]	34.6	0.37	98	TE_{01}□	1000	34	52	3.5	0.85(4.0)	Ind. LINAC	0.02	amplifier
[66]	140	0.17	98	TE_{11}○	2000	13.3	58	6.0	2.5 (3.0)	Ind. LINAC	0.02	amplifier
MIT, Cambridge [45,67]	9.3	0.02	33	TE_{11}○	0.1	10	6	0.18	0.0055	Electrostatic	0.02	amplifier
	27.5	0.05	30	TE_{11}○	1	10.3	-	0.32	0.03(0.05)	Electrostatic	1	oscillator
	33.4	0.15	32	TE_{11}○	61	27	50	0.75	0.3	Electrostatic	0.03	amplifier
	35.2	0.05	30	TE_{11}○	0.8	8.6	26	0.31	0.03(0.05)	Electrostatic	1	amplifier
NRL,WashingtonD.C.[68]	12.5-16.5	0.1	30	TE_{01}□	0.7	3		0.25	0.1			amplifier
	23-31	0.06	40	TE_{01}○	4	3		0.7	0.2	Ind. LINAC	0.035	amplifier
	35	0.14	30	TE_{11}○	17	3.2	50	0.9	0.6	Pulse Line	0.02	amplifier
	75	0.08	30	TE_{11}○	75	6	50	1.25	1.0	Pulse Line	0.02	amplifier
SIAE, Chengdu [75]	37	0.125	34.5	TE_{11}○	7.6	5.4		0.5	0.28	Electrostatic	0.015	oscillator
TRW, Redondo Beach [69]	35	0.16	20	TE_{01}□	0.1	9.2		0.3	0.004	Electrostatic	10	oscillator
	35	0.16	20	TE_{01}□	0.1	9.2	2	0.29	0.0001	Electrostatic	10	amplifier
UCSB Santa Barbara[70]	120-880	0.65	18.5		0.015	5		6	0.002	Electrostatic	20	oscillator

Table XI: State-of-the-art of millimeter- and submillimeter wave FEMs

10.3 The FOM-Fusion FEM

A free electron maser is being designed at the FOM Institute "Rijnhuizen" for ECRH applications on future fusion devices [72]. The FEM will have an output power of 1 MW, a central frequency of 200 GHz and will be adjustable over the complete frequency range of 130 GHz to 260 GHz. The FEM is driven by a thermionic electron gun. Fast tunability is achieved by variation of the terminal voltage of the 2 MeV electrostatic accelerator. The undulator and mmw system are located in a terminal at a voltage of 2 MV, inside a vessel at 7 bar (see Fig. 15). After interaction with the mm waves in the undulator, the energy of the electron beam will be recovered by means of a decelerator and a multi-stage depressed collector. The low emittance electron beam will be completely straight to minimize current losses to less than 20 mA. This current is to be delivered by the 2 MV dc accelerating voltage power supply. Simultations indicate that the overall efficiency should be over 50 %.

The FOM-FEM will be an oscillator, consisting of a waveguide amplifier section and a feedback system (see Fig. 15). For the oversized waveguide inside the undulator a rectangular corrugated HE_{11} waveguide is chosen with a cross section of 15 x 20 mm^2. Directly behind the undulator the mm waves will be separated from the electron beam by means of a stepped waveguide. Here the width of the waveguide changes step-wise. Because of this step, the initial HE_{11} beam is splitted into two identical HE_{11} beams at about 1.5 m from the step. At this position two mirrors can be located with a hole in between, large enough to let the electron beam pass without disturbing the mmw beams (see Fig. 16). The two mmw beams at the location of the mirror are reflected with adjustable phases by changing the position of the mirrors. This enables a 0-100 % variation of the reflection coefficient (the fraction of the power that goes back through the interaction waveguide to the input side of the undulator, where a similar 100 % reflector is located). See Fig. 17 and 18. The remaining power is evenly divided over two output beams, these can be recombined to make the 1 MW output. Low-power measurements on a prototype separation system are very encouraging. The width of the waveguide a (after the step) is given by $a = \sqrt{2\lambda L}$, where L is the length of the electron-beam/mmw splitter: 1.5 m. At present a system is being designed to move the sidewalls of the splitter in order to optimize the dimension a for all frequencies from a = 60 mm for 260 GHz to a = 85 mm for 130 GHz. This system enables to vary the frequency over the complete range of 130 to 260 GHz by just changing the accelerator voltage, the splitter width and the reflection coefficient. All this can be controlled remotely. Table XII summarizes the design parameters of the planned FOM-FEM experiment.

Detailed simulations which take into account the propagation of the millimeter wave beam in the cavity and the interaction with the electron beam show that 99.8 % of the rf power is in the HE_{11} mode.

Transport of the mm waves to earth potential is done quasi-optically through a tube similar to the acceleration tube. By this method of transport a vacuum window at a pressure of 7 bar can be avoided.

Since frequency tuning is an important feature of the FEM, the output window has to be broadband, as well. Some promising solutions are discussed in [34].

1 MW, 130-250 GHz FOM-Fusion-FEM

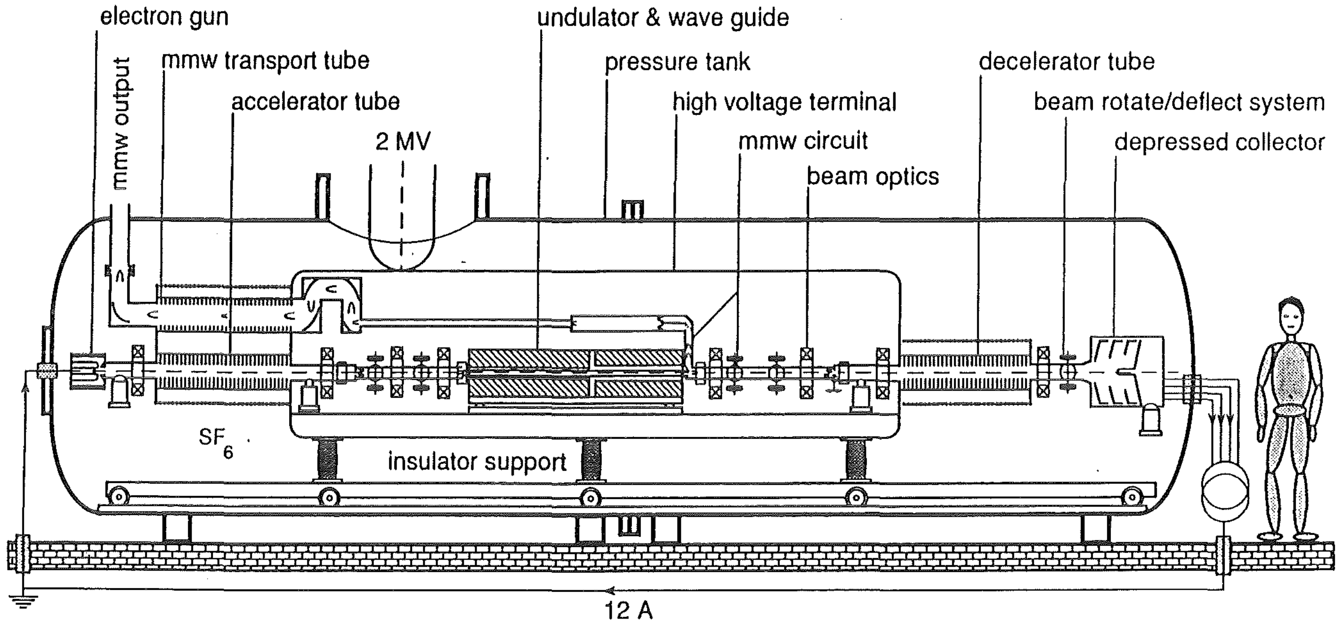

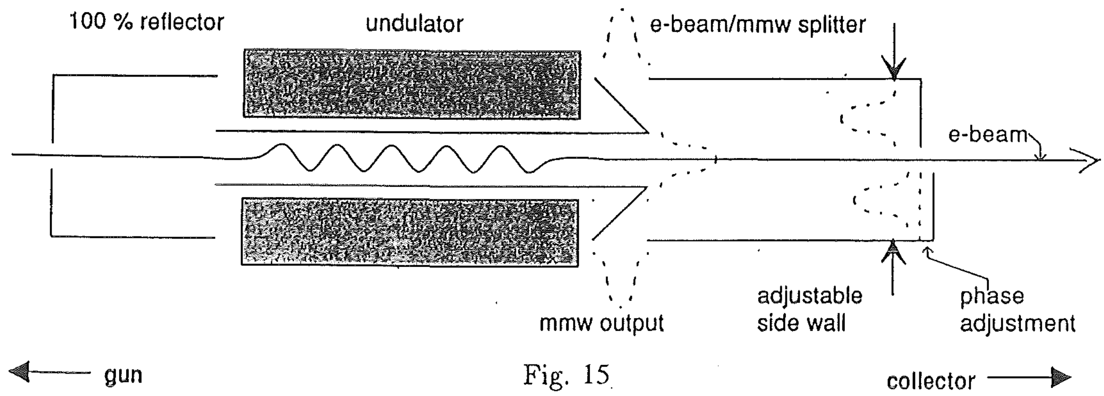

Fig. 15
The mmw system

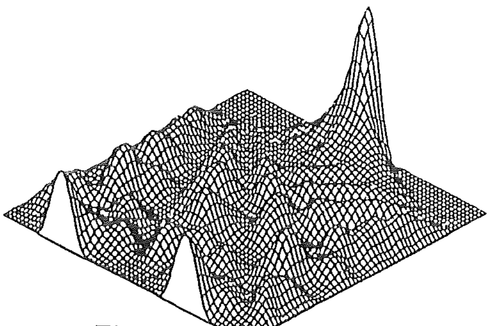

Fig. 16
Splitting of one HE_{11} beam into 2 beams

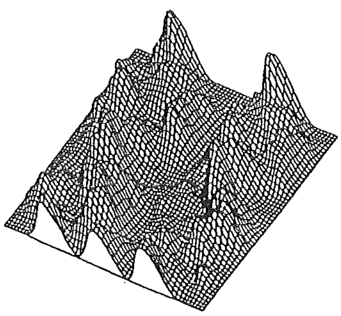

Fig. 17
Two beams are tranformed into 3 beams at a phase shift of 0.63π

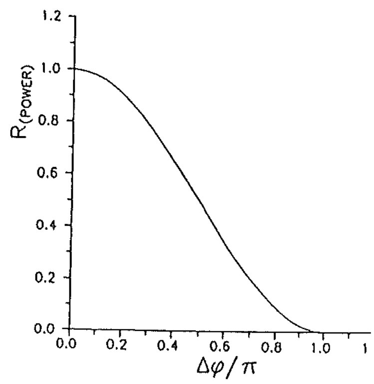

Fig. 18
Reflection coefficient vs phase shift

• power	1 MW - sufficient for FEM demonstration - comparable with biggest gyrotrons
• center frequency	130 GHz, 200 GHz, 250 GHz - future use on fusion devices - higher than gyrotron frequencies
• ms-scale tunability	10 % via e-beam energy (high-voltage) - to demonstrate advantage of FEM - for tracking of plasma disruptions
• gain	3 (saturation) - to limit intra-cavity power ≈ 7 (small signal gain) - fast start-up (≈ 1 μs)
• extraction eff., η	5 %
• pulse duration	100 ms - eventually CW but at first 100 ms to avoid severe colling problems
• power efficiency	≈ 60 % (grid --> millimeter wave power)
• electron beam	12A, @ V= 2.0, 1.75, 1.35 MeV for f = 250, 200, 130 GHz
• undulator	- period = 40 mm, 2 sections - section 1: 20 cells, B= 0.20 T - gap: 25 mm - section 2: 14 cells, B= 0.16 T

Table XII: Design parameters of the planned FOM-FEM [70]

11 Comparison of gyrotron and FEM for nuclear fusion

Table XIII lists a comparison of the main performance parameters and features of gyrotron oscillators and FEMs for ECRH of plasmas in nuclear fusion research. The important advantage of the FEM is its fast and continuous frequency tunability and the possibility of high unit power but the gyromonotron is the much simpler device. Up to now, the cylindrical cavity gyrotron is the only millimeter wave source which has gained an extensive on-the-field experience during ECRH experiments over a wide range of frequencies and power levels (28-140 GHz, 0.1-0.5 MW).

	Gyrotron Oscillator (cyclotron resonance maser axial magnetic field)	Free Electron Maser Oscillator (periodic transverse magnetic field)
1. Beam voltage	low (70 - 90kV)	high (0.2 - 2 MV)
2. Magnetic field (140 GHz)	high (5.5 T, 1st harmonic)	low (0.2 T, wiggler)
3. Frequencies	8 - 250 GHz	9 - 250 GHz
4. Frequency tunability	ΔB: slow step tuning $\Delta U_{beam} + \Delta U_{mode}$: fast step tuning (few steps)	ΔU_{beam}: fast continuous tuning (10%)
5. Electron beam	magnetron injection gun	Pierce electron gun, acceleration and deceleration tubes, beam optics
6. Ohmic losses in cavity	cutoff cavity 2 kW/cm^2	oversized circuit far away from cutoff
7. Power density in cavity	high	low
8. Longitudinal mode competition in cavity	single mode operation	nonlinear temporal dynamics can bring broad frequency spectrum (noise source?)
9. Linearly polarized output mode	generated by internal quasi-optical converter	linearly polarized, low-order resonator mode
10. Power density on first mirror (1 MW, 140 GHz)	1 kW/cm^2	2kW/cm^2
11. Number of internal quasi-optical mirrors	2-3	4-14 phase coherence required
12. Internal microwave diagnostics	not required	required
13. Output power present status (140 GHz)	high average power 0.6 MW/2s	2GW/20ns but very low duty cycle (LLNL amplifier)
14. Exp. system efficiency without energy recovery	high 30-40 %	low 5-10 %
15. Collector loading	relatively low	high
16. Theor. system efficiency with depressed collector	55 %	55 % (but halo current ?)
17. Physical size	relatively small	large
18. Power per unit (140 GHz)	1-2 MW	1-5 MW

Table XIII: Comparison of parameters and features of gyrotron oscillators and FEMs for ECRH.

Acknowledgments

This work was performed under the auspices of the Project Nuclear Fusion (Projekt Kernfusion) at the Kernforschungszentrum Karlsruhe.

The author wishes to thank E. Borie, O. Dumbrajs, G. Gantenbein, H.-U. Nickel and B. Piosczyk for stimulating discussions and critical reading of the manuscript.

References

[1] Flyagin, V.A., Nusinovich, G.S., 1988, Gyrotron oscillators. Proceedings of the Institute of Electrical and Electronics Engineers, **76**, 644-656.

[2] Felch, K., Huey, H., Jory, H., 1990, Gyrotrons for ECH application. J. Fusion Energy, **9**, 59-75.

[3] Döring, H., 1986, Stand der Gyrotronentwicklung, NTG-Fachberichte 95, Elektronenröhren und Vakuumelektronik, Garmisch Partenkirchen, VDE-Verlag GmbH, 1986.

[4] Prater, R., 1990, Recent results on the application of electron cyclotron heating in tokamaks. J. Fusion Energy, **9**, 19-30.

[5] Erckmann, V., WVII-AS Team, Kasparek, W., Müller, G.A., Schüller, P.G., and Thumm, M., 1990, Electron cyclotron resonance heating transmission line and launching system for the Wendelstein VII-AS stellarator. Fusion Technology, **17**, 76-85.

[6] Henle, W., Jacobs, A., Kasparek, W., Kumric, H., Müller, G.A., Schüller, P.G., Thumm, M., Engelmann, F., Rebuffi, L., 1991, Conceptual study of multi-megawatt millimeter wave transmission and antenna systems for electron cyclotron wave applications in NET/ITER. Fusion Technology,**1990**, eds. B.E. Keen, M. Huguet, R. Hemsworth. Elsevier Science Publishers B.V., 238-242.

[7] Alberti, S., Tran, M.Q., Hogge, J.P., Tran, T.M., Bondeson, A., Muggli, P., Perrenoud, A., Jödicke, B., Mathews, H.G., 1990, Experimental measurements on a 100 GHz frequency tunable quasi-optical gyrotron. Phys. Fluids, **B2**, 1654-1661.

[8] Kreischer, K.E. Temkin, R.J., 1987, Single-mode operation of a high-power, step-tunable gyrotron. Phys. Rev. Lett., **59**, 547-550.

[9] Kurbatov, V.I., Malygin, S.A., Vasilyev, E.G., 1990, Commercial gyrotrons for thermonuclear investigations. Proc. Int. Workshop on Strong Microwaves in Plasmas, Suzdal, Inst. of Applied Physics, Nizhny Novgorod, 1991, 765-772.
Bogdanov, S.D., Kurbatov, V.I., Malygin, S.A., Orlov, V.B., Tai, E.M., 1993, Industrial gyrotrons development in Salut. Proc. 2nd Int. Workshop on Strong Microwaves in Plasmas, Nizhny Novgorod, Contributed Paper S42.

[10] Flyagin, V.A., Kuftin, A.N., Luchinin, A.G., Nusinovich, G.S., Pankratova, T.B., Zapevalov, V.E., 1989 , Gyrotrons for electron cyclotron heating and active plasma diagnostics. Proc. Joint IAEA Techn. Committee Meeting on ECE and ECRH (EC-7 Joint Workshop), Hefei, P.R. China, 355-372.

[11] Bykov, Y., Goldenberg, A.F.L., Flyagin, V.A., 1991, The possibilities of material processing by intense millimeter-wave radiation. Mat. Res. Soc. Symp. Proc., **169**, 41-42.
Sklyarevich, V., Detkov, A., Shevelev, M., Decker, R., 1992, Mat. Res. Soc. Symp. Proc., **269**, 163-169.

[12] Granatstein, V.L., Lawson, W., Latham, P.E., 1988, Feasibility of 30 GHz gyroklystron amplifiers for driving linear supercolliders, Conf. Digest, 13th Int. Conf. on Infrared and Millimeter Waves, Honolulu, Hawaii, SPIE Vol., **1039**, 230-231.

[13] Bratman, V.L., Denisov, G.G., Ginzburg, N.S., and Petelin, M.I., 1983, FEL's with Bragg reflection resonators. Cyclotron autoresonance masers versus ubitrons. I.E.E.E. Journal Quantum Electronics, **QE-19**, 282-296.

[14] Orzechowski, T.J., Anderson, B.R., Clark, J.G., Fawley, W.M., Paul, A.C., Prosnitz, D., Scharlemann, E.T., Yarema, S.M., Hopkins, D.B., Sessler, A.M., Wurtele, J.S., 1986, High-efficiency extraction of microwave radiation from a tapered-wiggler free-electron laser. Phys. Rev. Lett., **57**, 2172-2175.

[15] Stone, R.R., Jong, R.A., Orzechowski, T.J., Scharlemann, E.T., Throop, A.L., Kulke, B., Thomassen, K.I., Stallard, B.W., 1990, An FEL-based microwave system for fusion. J. Fusion Energy, **9**, 77-101.

[16] Granatstein, V.L., Alexeff, I., eds., 1987, High-power microwave sources. Artech House, Boston, London.

[17] Pendergast, K.D., Danly, B.G., Menninger, W.L., Temkin, R.J.,1992, A long-pulse CARM oscillator experiment. Int. J. Electronics, **72**, 983-1004.

[18] Mathews, H.-G., Tran, M.Q., 1991, private communication, ABB, Baden, Switzerland.

[19] Chen, Z.-G., 1992, private communication, Institute of Electronics, Academica Sinica (IEAS), Beijing, P.R. China and Guo, H., Wu, D.S., Liu, G., Miao, Y.H., Qian, S.Z., Qin, W.Z., 1990, Special complex open-cavity and low-magnetic field high power gyrotron, IEEE Trans. on Plasma Science, **PS-18**, 326-333.

[20] Mourier, G., 1990, Current gyrotron development at Thomson Tubes Electroniques Proc. Int. Workshop on Strong Microwaves in Plasmas, Suzdal, Inst. of Applied Physics, Nizhny Novgorod, 1991, 751-764 and, 1993, private communication.

[21] Nagashima, T., Sakamoto, K., Maebara, S., Tsuneoka, M., Okazaki, Y., Hayashi, K., Miyake, S., Kariya, T., Mitsunaka, Y., Itoh, Y., Sugawara, T., Okamoto, T., 1990, Test results of 0.5 MW gyrotron at 120 GHz and 1.5 MW at 2 GHz Klystron for fusion application. Proc. Int. Workshop on Strong Microwaves in Plasmas, Suzdal, Inst. of Applied Physics, Nizhny Novgorod, 1991, 739-750.

[22] Felch, K., Chu, T.S., Feinstein, J., Huey, H., Jory, H., Nielson, J., Schumacher, R., 1992, Long-pulse operation of a gyrotron with beam/rf separation. Conf. Digest 17th Inf. Conf. on Infrared and Millimeter Waves, Pasadena, Proc., SPIE **1929**, 184-195.
Lawrence Ives, R., Jory, H., Neilson, J., Chodorow, M., Feinstein, J., LaRue, A.D., Zitelli, L., Martorana, R., 1993, Development and test of a 500 kW, 8-GHz Gyrotron. IEEE Trans. on Electron Devices, **40**, 1316-1321.

[23] Thumm, M., 1986, High power mode conversion for linearly polarized HE11 hybrid mode output. Int. J. Electronics, **61**, 1135-1153.

[24] Piosczyk, B., Kuntze, M., Borie, E., Dammertz, G., Dumbrajs, O., Gantenbein, G., Möbius, A., Nickel H.-U., Thumm, M., 1993, Fusion Technology **1992**, Development of high power 140 GHz gyrotrons at KfK for applications in fusion, eds. C. Ferro, M. Gasparotto, H. Knoepfel. Elsevier Science Publishers B.V., 618-622.
Borie, E., Dammertz, G., Gantenbein, G., Kuntze, M., Möbius, A., Nickel, H.-U., Piosczyk, B., Thumm, M., 1993, 0.5 MW/140 GHz $TE_{10,4}$ Gyrotron with built-in highly efficient quasioptical converter, Conf. Digest 18th Int. Conf. on Infrared and Millimeter Waves, Colchester (Essex, UK), Proc., SPIE **2104**, 519-520.

[25] Shimozuma, T., Kikunaga, T., Asano, H., Yasojima, Y., Miyamoto, K., Tsukamoto, T., 1993, A 120 GHz high-power whispering-gallery mode gyrotron. Int. J. Electronics, **74**, 137-151.

[26] Sakamoto, K, Tsuneoka, M., Maebava, S., Kasugai, A., Fujita, H., Kikuchi, M., Yamamoto, T., Nagashima, T., Kariya, T., Okazaki, Y, Shirai, N., Okamoto, T. Hayashi, K., Mitsunaka, Y., Hirata, Y., 1992, Development of a high power gyrotron for ECH of tokamak plasma. Conf. Digest 17th Int. Conf. on Infrared and Millimeter Waves, Pasadena, SPIE **1929**, 188-189.
Sakamoto, K., Tsuneoka, M., Kasugai, A., Maebara, S., Nagashima, T., Imai, T., Kariya, T., Okazaki, Y., Shirai, N., Okamoto, T., Hayashi, K., Mitsunaka, Y., Hirata, Y., 1993, Development of a high power gyrotron for fusion application in JAERI. Proc. 2nd Int. Workshop on Strong Microwaves in Plasmas, Nizhny Novgorod, Invited Paper S4.

[27] Myasnikov, V.E., Cayer, A.P., Bogdanov, S.D., Kurbatov, V.I., 1991, Soviet industrial gyrotrons. Conf. Digest 16th Int. Conf. on Infrared and Millimeter Waves, Lausanne, SPIE, **1576**, 127-128.

[28] Gantenbein, G., Borie, E., Möbius, A., Piosczyk, B., 1991, Design of a high-power 140 GHz gyrotron oscillator operating in an asymmetric volume mode at KfK. Conf. Digest 16th Int. Conf. on Infrared and Millimeter Waves, Lausanne, SPIE, **1576**, 264-265.

[29] Flyagin, V.A., Goldenberg, A.L., Zapevalov, V.E., 1993, State of the art of gyrotron investigation in Russia, Conf. Digest 18th Int. Conf. on Infrared and Millimeter Waves, Colchester (Essex, UK), Proc., SPIE **2104**, 581-584.

Denisov, G.G., Flyagin, V.A., Goldenberg, A.L., Khizhnyak, V.I., Kuftin, A.N., Malygin, V.I., Pavelyev, A.B., Pylin, A.V., Zapevalov, V.E., 1991, Investigation of gyrotrons in IAP. Conf. Digest 16th Int. Conf. on Infrared and Millimeter Waves, Lausanne, SPIE, **1576**, 632-635.

[30] Denisov, G.G., Kuftin, A.N., Malygin, V.I., Venediktov, N.P., Vinogradov, D.V., Zapevalov, V.E., 1992, 110 GHz gyrotron with a built-in high-efficiency converter, Int. J. Electronics, **72**, 1079-1091.

[31] Xu, K.Y., Kreischer, K.E., Guss, W.C., Grimm, T.L., Temkin, R.J., 1990, Efficient operation of a megawatt gyrotron. Conf. Digest 15th Int. Conf. on Infrared and Millimeter Waves, Orlando, SPIE, **1514**, 324-326.

[32] Dumbrajs, O., Nusinovich, G.S., 1992, Theory of a frequency-step-tunable gyrotron for optimum plasma ECRH. IEEE Trans. Plasma Science, **20**, 452-457.

[33] Petelin, M.I., Kasparek, W., 1991, Surface corrugation for broadband matching of windows in powerful microwave generators. Int. J. Electronics, **71**, 871-873.

[34] Nickel, H.-U., Ambrosy, U., Thumm, M., 1992, Vacuum windows for frequency-tunable high-power millimeter wave systems. Conf. Digest 17th Int. Conf. on Infrared and Millimeter Waves, Pasadena, Proc., SPIE **1929**, 462-463.

Nickel, H.-U., Massler, H., Thumm, M., 1993, Development of broadband vacuum windows for high-power millimeter wave systems. Conf. Digest 18th Int. Conf. on Infrared and Millimeter Waves, Colchester (Essex, UK), Proc., SPIE **2104**, 172-173.

Shang, C.C., Caplan, M., Nickel, H.-U., Thumm, M., 1993, Electrical analysis of wideband and distributed windows using time-dependent field codes, Conf. Digest 18th Int. Conf. on Infrared and Millimeter Waves, Colchester (Essex, UK), Proc., SPIE **2104**, 178-179.

[35] Kreischer, K.E., Grimm, T.L., Guss, W.C., Temkin, R.J., Xu, K.Y, 1990, Research at MIT on high frequency gyrotrons for ECRH. Proc. Int. Workshop on Strong Microwaves in Plasmas, Suzdal, Inst. of Applied Physics, Nizhny Novgorod, 1991, 713-725.

[36] Grimm, T.L., Borchard, P.M., Kreischer, K.E., Guss, W.C., Temkin, R.J., 1992, High power operation of a 200-300 GHz gyrotron oscillator and multimegawatt gyrotrons for ITER. Conf. Digest 17th Int. Conf. on Infrared and Millimeter Waves, Pasadena, SPIE **1929**, 190-191 and 194-195.

Grimm, T.L., Kreischer, K.E., Guss, W.C., Temkin, R.J., 1992, Experimental study of a megawatt 200-300 GHz gyrotron oscillator, Fusion Technology, **21**, 1648-1657.

[37] Zaytsev, N.I., Pankratova, T.P., Petelin, M.I., Flyagin, V.A., 1974, Millimeter- and submillimeter-wave gyrotrons. Radio Eng. and Electronic Phys., **19**, 103-107.

[38] Idehara, T., Tatsukawa, T., Ogawa, I., Tanabe, H., Mori, T., Wada, S., Brand, G.F., Brennan, M.H., 1992, Development of a second cyclotron harmonic gyrotron operating at submillimeter wavelengths, Phys. Fluids **B4**, 267-273 and 1993, Phys. Fluids **B5**, 1377-1379.

Idehara, T., Tatsukawa, T., Ogawa, I., Shimizu, Y., Makino, S., Ichikawa, K., 1993, Development of medium power, submillimeter wave gyrotrons, Conf. Digest 18th Int. Conf. on Infrared and Millimeter Waves, Colchester (Essex, UK), Proc., SPIE **2104**, 533-534.

[39] Brand, G.F., Fekete, P.W., Hong, K., Moore, K.J., Idehara, T., 1990, Operation of a tunable gyrotron at the second harmonic of the electron cyclotron frequency. Int. J. Electronics, **68**, 1099-1111.

[40] Spira, S.E., Kreischer, K.E., Temkin, R.J., 1988, Operation of harmonic gyrotrons in the submillimeter region. Conf. Digest 13th Int. Conf. Infrared and Millimeter Waves, Honolulu, SPIE, **1039**, 429-430.

[41] Geist, T., Thumm, M., Wiesbeck, W., 1991, Linewidth measurement on a 140 GHz gyrotron. Conf. Digest 16th Int. Conf. on Infrared and Millimeter Waves, Lausanne, SPIE, **1576**, 272-273.

[42] Fliflet, A.W., Hargreaves, T.A., Fischer, R.P., Manheimer, W.M., Sprangle, P., 1990, Review of quasi-optical gyrotron development. J. Fusion Energy, **9**, 31-58.
Fischer, R.P., Fliflet, A.W., Manheimer, W.M., Levush, B., Antonsen Jr., T.M., 1993, Mode priming an 85 GHz quasioptical gyroklystron, Conf. Digest 18th Int. Conf. on Infrared and Millimeter Waves, Colchester (Essex, UK), Proc., SPIE **2104**, 330-331.

[43] Hogge, J.P., Cao, H., Kasparek, W., Tran, T.M., Tran, M.Q., Paris, P.J., 1991, Ellipsoidal diffraction grating as output coupler for quasi-optical gyrotrons. Conf. Digest 16th Int. Conf. on Infrared and Millimeter Waves, Lausanne, SPIE, **1576**, 540-541.

[44] Bratman, V.L., Denisov, G.G., 1992, Cyclotron autoresonance masers - recent experiments and prospects. Int. J. Electronics, **72**, 969-981.
Bratman, V.L., 1993, Cyclotron autoresonance masers: achievements and prospects of advance to the submillimeter wavelength range, Proc. 2nd Int. Workshop on Strong Microwaves in Plasmas, Nizhny Novgorod, Invited Paper S9.

[45] Danly, B.G., Hartemann, F.V., Chu, T.S., Legorburn, P., Menninger, W.L, Temkin, R.J., 1992, Long-pulse millimeter-wave free-electron laser and cyclotron autoresonance maser experiments. Phys. Fluids, **B4**, 2307-2314.

[46] Wang, J.G., Gilgenbach, R.M., Choi, J.J., Outten, C.A., Spencer, T.A., 1989, Frequency-tunable, high-power microwave emission from cyclotron autoresonance maser oscillation and gyrotron interactions. IEEE Trans. Plasma Science, **17**, 906-908.

[47] Caplan, M., Kulke, B., Westenskow, G.A.; McDermott, D.B., Luhmann, Jr.,N.C., 1992, Induction-linac-driven, millimeter-wave CARM oscillator, Exploratory Research and Development, **FY 90**, 146-147.

[48] Burke, J.M., Czarnaski, M.A., Fischer, R.P., Giangrave, M., Fliflet, A.W., Manheimer, W.M., 1991, 85 GHz TE13 phase-locked gyroklystron oscillator experiment. Conf. Digest 16th Int. Conf. on Infrared and Millimeter Waves, Lausanne, SPIE, **1576**, 228-229.

[49] Fischer, R.P., Fliflet, A.W., Manheimer, W.M., 1992, The NRL 85 GHz quasioptical gyroklystron experiment, Conf. Digest 17th Int. Conf. on Infrared and Millimeter Waves, Pasadena, SPIE **1929**, 254-255.

[50] Chu, K.R., Barnett, L.R., Lau, W.K., Chang, L.H., Chen H.Y.,1990, A wide-band millimeter-wave gyrotron traveling-wave amplifier experiment. IEEE Trans.Electron Devices, **37**, 1557-1560.

[51] Park, G.S., Park, S.Y., Kyser, R.H., Armstrong, C.M., Ganguly, A.K., Parker, R.K., 1991, Experimental study of a broadband millimeter-wave gyrotron traveling wave amplifier. Conf. Digest 16th Int. Conf. on Infrared and Millimeter Waves, Lausanne, SPIE, **1576,** 198-199.

[52] Tantawi, S.G., Main, W.T., Latham, P.E., Nusinovich, G.S., Lawson, W.G., Striffler, C.D., Granatstein, V.L., 1992, High-power X-band amplification from an overmoded three-cavity gyroklystron with a tunable penultimate cavity. IEEE Trans. on Plasma Science, **PS-20**, 205-215.

[53] Lawson , W., Calame, J.P., Hogan, P., Skopec, M., Striffler, C.D., Granatstein, V.L., 1992, Performance characteristics of a high-power X-band two-cavity gyroklystron. IEEE Trans. on Plasma Science, **PS-20**, 216-223.
Lawson, W., Matthews, H.W., Lee, M.K.E., Hogan, B., Calame, J.P., Cheng, J., 1993, High power operation of a K-band second harmonic gyroklystron, Conf. Digest 18th Int. Conf. on Infrared and Millimeter Waves, Colchester (Essex, UK), Proc., SPIE **2104**, 527-528.

[54] Park, G.-S., Granatstein, V.L., Park, S.Y., Armstrong, C.M., Ganguly, A.K., 1992, Experimental study of efficiency optimization in a three-cavity gyroklystron amplifier. IEEE Trans. on Plasma Science, **PS-20**, 224-231.

[55] Antakov, I.I., Aksenova, L.A., Zasypkin, E.V., Moisseev, M.A., Popov, L.G., Sokolov, E.V., Yulpatov, V.K., 1990, Mulit-cavity phase-locked gyrotrons for lower-hybrid heating in torodial plasmas. Proc. Int. Workshop on Strong Microwaves in Plasmas, Suzdal, Inst. of Applied Physics, Nizhny Novgorod, 1991, 773-782.

[56] Antakov, I.I., Moiseev, M.A., Sokolov, E.V., Zasypkin, E.V., 1993, Theoretical and experimental investigation of X-band two-cavity gyroklystron, Conf. Digest 18th Int. Conf. on Infrared and Millimeter Waves, Colchester (Essex, UK), Proc., SPIE **2104**, 336-337.

Antakov, I.I., Zasypkin, E.V., Sokolov, E.V., Yulpatov, V.K., Keyer, A.P., Musatov, V.S., Myasnikov, V.E., 1993, 35 GHz radar gyroklystrons, Conf. Digest 18th Int. Conf. on Infrared and Millimeter Waves, Colchester (Essex, UK), Proc., SPIE **2104**, 338-339.

Anatokov, I.I., Zaspykin, E.V., Sokolov, E.V., 1993, Design and performance of 94 GHz high power multicavity gyroklystron amplifier, Conf. Digest 18th Int. Conf. on Infrared and Millimeter Waves, Colchester (Essex, UK), Proc., SPIE **2104**, 466-467.

[57] Park, S.Y., Kyser, R.H., Armstrong, C.M., Parker, R.K., Granatstein, V.L., 1990, Experimental Study of a Ka-band gyrotron backward-wave oscillator. IEEE Trans. on Plasma Science, **PS-18**, 321-325.

[58] Kou, C.S., Chen, S.H., Barnett, L.R., Chu, K.R., 1992, Experimental study of an injection locked gyrotron backward wave oscillator. Conf. Digest 17th Int. Conf. on Infrared and Millimeter Waves, Pasadena, SPIE **1929**, 387a.

[59] Guss, W.C., Basten, M.A., Kreischer, K.E., Temkin, R.J., Caplan, M., Kulke, B., 1989, Operation of a 140 GHz tunable backward-wave gyrotron oscillator. Conf. Digest 14th Int. Conf. on Infrared and Millimeter Waves, Würzburg, SPIE, **1240**, p. 83.

[60] Bizzarri, U., Ciocci, F., Dattoli, G., De Angelis, D. Dipace, A., Doria, A., Fiorentino, E., Giabbai, I., Giannessi, L., Giordano, G., Gallerano, G.P., Hermsen, T., Letardi, T., Marino, A., Mezi, L., Messina, G., Mola, A., Picardi, L., Renieri, A., Ronsivalle, C., Sbia, E., Schettini, G., Torre, A., Vignati, A., Jaroszynski, D.A., Kimmitt, M.F., Pidgeon, C.R., 1988, Status of the undulator magnet FEL activity at the ENEA Frascati Center, Proc. of "EUROLASER One-Day Informal Workshop Workshop on FEL", A. Renieri ed., ENEA Franscati (Italy), 135-143.

[61] Doria, A., Gallerano, G.P., Giovenale, E., Kimmitt, M.F., Messina, G., Renieri, A., 1993, The ENEA compact millimeter wave FEL, Conf. Digest 18th Int. Conf. on Infrared and Millimeter Waves, Colchester (Essex, UK), Proc., SPIE **2104**, 17-18.

Ciocci, F., Bartolini, R., Doria, A., Gallerano, G.P., Giovenale, E., Kimmitt, M.F., Messina, G., Renieri, A., 1992, First operation of a compact FEL in the millimeter wave region, Conf. Digest 17th Int. Conf. on Infrared and Millimeter Waves, Pasadena (Los Angeles), Proc. SPIE **1929**, 52-53.

[62] Hartemann, F., Buzzi, J.M., 1988, Experimental studies of a millimeter-wave free-electron laser, Proc. 7th Int.Conf. on High-Power Particle Beams, Karlsruhe 1988, eds., Bauer, W., Schmidt, W., Vol. II, 1278-1292.

[63] Van Amersfoort, P.W., Bakker, R.J., Bekkers, J.B., Best, R.W.B., van Buuren, R., Delmee, P.F.M., Faatz, B., Van der Geer, C.A.J., Jaroszynski, D.A., Manintveld, P., Mastop, W.J., Meedens, B.J. H., van der Meer, A.F.G., Nijman, J.P., Oept, D., Pluygers, J., van der Wiel, M.J., Gillespie, W.A., Marin, P.F., Kimmitt, M.F., Pidgeon, C.R., Poole, M.W., Saxon, G., 1992, First Lasing with FELIX, Nucl. Instr. and Methods in Phys. Research, **A318**, 42-46.

[64] Ohkuma, J., Okuda, S., Tsumori, K., 1991, Measurement of coherent cherenkov radiation from an intensive beam of a picosecond electron bunch, Phys. Rev. Lett. **66**, 1967-1969.

[65] Sakamoto, K., Kishimoto, Y., Watanabe, A., Kobayashi, T., Musyoki, S., Oda, H., Tokuda, S., Nakamura, Y., Kawasaki, S., Ishizuka, H., Sato, M., Nagashima, T., Shiho, M., 1992, MM wave FEL experiment with focusing wiggler, Course and Workshop on High Power Microwave Generation and Applications, Int. School of Plasma Physics, Varenna, 1991, eds., D. Akulina, E. Sindoni, C. Wharton, Editrice Compositori Bologna, 597-604.
Sakamoto, K., Shiho, M., Musyoki, S., Watanabe, A., Kishimoto, Y., Kawasaki, S., Ishizuka, H., 1993, Study of waveguide mode identification in FEL experiment. Proc. 15th Int. Free Electron Laser Conference, The Hague, The Netherlands, Paper Mo 4-16.

[66] Allen, S.L., Casper, T.A., Fenstermacher, M.E., Foote, J.H., Hooper, E.B., Hoshino, K., Lasnier, C.J., Lopez, P., Makowski, M.A., Marinak, M.M., Meyer, W.H., Moller, J.M., Oasa, K., Oda, T., Odajima, K., Ogawa, T., Ogo, T., Rice, B.W., Rognlien, T., Stallard, B.W., Thomassen, K.I., Wood, R.D., 1992, Electron cyclotron resonance heating in the microwave tokamak experiment. 14th Int. Conf. on Plasma Physics and Controlled Nuclear Fusion Research, Würzburg, IAEA-CN-56/E-1-4.

[67] Conde, M.E., Bekefi, G., 1992, Amplification and superradiant emission from a 33.3 GHz free electron laser with a reversed axial guide magnetic field. IEEE Trans. Plasma Science, **20**, 240-244.

[68] Pasour, J.A., Gold, S.H., 1985, Free electron laser experiments with and without a guide magnetic field: a review of millimeter-wave free electron laser research at the NRL, IEEE J. Quantum Electronics, **QE-21**, 845-858.

[69] Boehmer, H., Christensen, T., Camponi, M.Z., Hauss, B., 1990, A long-pulse millimeter-wave free electron maser experiment. IEEE Trans. Plasma Science, **18**, 392-398.

[70] Elias, L.R., Ramian, G., Hu, J., Amir, A. 1986, Observation of single mode operation of a free electron laser . Phys. Rev. Lett., **57**, 424-427.

[71] Leou, K.C., Wang, Q.S., Chong, C.K., Balkcum, A.J., Fochs, S.N., Garland, E.S., Pretterebner, J., Lin, A.T., McDermott, D.B., Hartemann, F., Luhmann, Jr., N.C., 1993, Gyro-TWT amplifiers at UCLA, Conf. Digest 18th Int. Conf. on Infrared and Millimeter Waves, Colchester (Essex, UK), Proc., SPIE **2104**, 531-532.
Leou, K.C., McDermott, D.B., Luhmann, Jr., N.C., 1992, Design of experimental dielectric loaded wideband Gyro-TWT. Conf. Digest 17th Conf. on Infrared and Millimeter Waves, Pasadena, Proc., SPIE **1929**, 326-327.

[72] Verhoeven, A.G.A., Bongers, W.A., Best, R.W.B., van Ingen, A.M., Manintveld, P., Urbanus, W.H., van der Wiel, M.J., Bratman, V.L., Denisov, G.G., Shmelyov, M.Yu., Nickel, H.-U., Thumm, M., Müller, G., Kasparek, W., Pretterebner, J., Wagner, D., Caplan, M., 1992, The 1 MW, 200 GHz FOM-Fusion-FEM, Conf. Digest 17th Int. Conf. on Infrared and Millimeter Waves, Pasadena (Los Angeles), Proc. SPIE **1929**, 126-127.

[73] Ono, S., Yamanouchi, K., Shibata, Y., Koike, Y., 1962, Cyclotron fast-wave tube using spatial harmonic interaction- the traveling wave peniotron. Proc. 4th Int. Congress Microwave Tubes, Scheveningen, 355-363.

[74] Ganguly, A.K., Ahn, S., Park, S.Y., 1988, Three dimensional nonlinear theory of the gyropeniotron amplifier. Int. J. Electronics, **65**, 597-618.

[75] Liu, S., 1992, Recent development of FEL research activities in P.R. China, Conf. Digest 17th Int. Conf. on Infrared and Millimeter Waves, Pasadena, Proc., SPIE **1929**, 441 and private communication.